

MAGNETOHYDRODYNAMIC SURFACE WAVES

Thesis by

David P. Hoult

In Partial Fulfillment of the Requirements

For the Degree of

Doctor of Philosophy

California Institute of Technology

Pasadena, California

1962

## ACKNOWLEDGEMENTS

The author wishes to thank Professor H. W. Liepmann, thesis advisor, and Professors J. D. Cole and G. B. Whitham for their continued interest and helpful discussions on the theoretical parts of this thesis.

I wish to thank Mrs. Geraldine Krentler who has done an excellent job of preparing the typescript. Thanks to Mrs. Nell Kindig and Miss Dorothy Lodter for preparing the figures.

This work has been sponsored by the Office of Naval Research under contracts N-onr 220-21 and 220 (36).

## ABSTRACT

This is an experimental and theoretical study of deep water gravity-like waves which are induced in a liquid metal by a changing magnetic field. The dominant feature of such waves is the emission of Alfvén waves from the free surface. A linearized theory is derived and compared with experiments.

## TABLE OF CONTENTS

	PAGE
Acknowledgements	ii
Abstract	iii
Table of Contents	iv
List of Symbols	vi
I. Introduction	1
II. Deep Water Gravity Wave Theory	6
III. Theory of Magnetohydrodynamic Deep Water Waves	12
IV. Theory of the Limiting Case	20
V. Linearized Theory of the Solenoid Problem	23
VI. Experiments	27
VII. Discussion of Previous Work	29
APPENDIX I: Theory of Magnetohydrodynamic Surface Waves	
A. Introduction	33
B. An Initial Value Problem	38
C. The Limiting Case of Infinite Conductivity	45
D. The Functions $H(s, k)$ and $\sqrt{\frac{s^2 + sk^2/Rm}{\alpha^2 + s/Rm}}$	52
E. The Alfvén Wave Structure	56
F. The Surface Shape	62
G. Conclusions	64
APPENDIX II: The Limiting Case $Rm \rightarrow 0$ , $\alpha^2 Rm \sim 1$	
The Response to a Pressure Pulse	67



## TABLE OF CONTENTS (Contd.)

	PAGE
APPENDIX III: The Solenoid Problem	76
APPENDIX IV: Experiments	
A. Introduction	86
B. Description of Data	89
C. Comparison of Theory and Experiment	91
References	98
Table I	99
Figures	100

## LIST OF PRINCIPAL SYMBOLS

(In Order of Appearance)

$\sigma$	electrical conductivity
$\mu$	magnet permeability
$\rho$	density
$B_0$	initial or final field strength
$\nu$	kinematic viscosity
$T$	surface tension
$g$	acceleration due to gravity
$a$	radius of solenoid
$Re$	Reynolds number
$\lambda$	wave length
$k$	wave number
$V_D$	diffusion speed
$V_A$	Alfvén speed
$V_G$	gravity speed
$Rm$	magnetic Reynolds number
$\alpha$	Alfvén number
$\zeta_0$	maximum surface amplitude
$(r, \theta, z)$	cylindrical coordinates, meters
$(\vec{l}_r, \vec{l}_\theta, \vec{l}_z)$	cylindrical unit vectors
$I$	solenoid current
$(B_r, 0, B_z)$	cylindrical magnetic field components
$t$	time
$P$	pressure

## LIST OF PRINCIPAL SYMBOLS (Contd.)

$(x, y, z)$	Cartesian coordinates
$(\vec{i}_x, \vec{i}_y, \vec{i}_z)$	Cartesian unit vectors
$\delta(x), \delta(t)$	Dirac delta functions
$\zeta(x, t)$	surface shape
$\lambda_0$	characteristic wave length
$\phi$	velocity potential
$s$	Laplace transform variable
$H(s, k)$	dispersion function
$k_0$	wave number at the point of stationary phase
$V_P$	phase velocity
$J_0(k_n r)$	Bessel function of the first kind of order zero
$k_n$	$n^{\text{th}}$ zero of $J_1(k_n) = 0$
$J_1(k_n)$	Bessel function of the first kind of order one
$\vec{b}$	nondimensional perturbation magnetic field
$\vec{e}$	nondimensional perturbation electric field
$\vec{j}$	nondimensional perturbation current density
$\vec{v}$	nondimensional perturbation velocity
$\vec{p}$	nondimensional perturbation pressure
$\vec{\omega}$	nondimensional perturbation vorticity
$( )^*, ( )^{\dagger}$	similarity variables
$A_m, \ell_m$	$m^{\text{th}}$ coefficient of Dini series
$c$	shallow water wave velocity

## LIST OF PRINCIPAL SYMBOLS (Contd.)

Appendix I

$A(x, z, t)$	magnetic vector potential
$\phi(x, z, t)$	harmonic function
$\widetilde{(\phi)}$	The Laplace and Fourier transform of $\phi$

Appendix II

$R = \alpha^2 R_m$	the parameter of the low conductivity limit
--------------------	---

Appendix III

$T$	physical time
$\bar{C}_m, \bar{E}_m$	Laplace transformed Dini series coefficients

Appendix IV

$\lambda$	rate of rise or decay of solenoid magnetic field
$\theta$	phase shift of surface responses
$\omega$	dimensional frequency
$\gamma$	dimensional damping factor
$A(T)$	amplitude factor
$\tau = \frac{\log 2}{\lambda}$	$\frac{1}{2}$ time of magnetic field

## I. Introduction

When a vertical cylindrical solenoid is half filled with mercury and the current to the solenoid is switched off or on, the free surface of the mercury is visually observed to be set into motion by the changing magnetic field. This thesis consists of theoretical and experimental studies based upon this observation.

We begin by trying to develop a model for the observed surface waves. Since the mercury column is 5 or 6 diameters long, we idealize the geometry to that of an infinitely long cylindrical solenoid half filled with mercury. Hence we assume that the bottom of the mercury column plays no role in the surface oscillations. This assumption will be verified later.

We have, as dimensional parameters of the problem (in MKSQ units), the conductivity  $\sigma$ , the magnetic permeability  $\mu$ , the density  $\rho$ , a magnetic field strength  $B_0$ , the kinematic viscosity  $\nu$ , the surface tension  $T$ , the acceleration due to gravity  $g$ , and the inner diameter of the solenoid  $2a$ . As is usual in magnetohydrodynamic problems, the displacement current is neglected.

In the present case,  $a = .071$  M, and  $\nu = 10^{-7}$  M<sup>2</sup>/S. Hence the Reynolds number based upon gravity speed is

$$Re = \sqrt{ga} \frac{a}{\nu} \approx 5 \times 10^5$$

Hence we may ignore viscous effects, and drop  $\nu$  from the list of relevant parameters.

We compute the minimum wave length,  $\lambda$ , of the combined gravity and capillary waves to be (for Hg,  $T = .480$  Newtons/meter,  $\rho = 13.54 \text{ Kg/M}^3$ ).

$$\lambda_{\min} \doteq 2\pi \sqrt{\frac{T}{\rho g}} \doteq .012 \text{ m}$$

This corresponds to a nondimensional wave number of

$$k_{\max} = \frac{2\pi a}{\lambda} \doteq 37$$

For wave numbers  $> k_{\max}$ , capillarity must be taken into account.

However, it will be shown below that the dominant wave number in the solenoid problem is given by

$$k_1 = 3.8$$

Hence we may neglect surface tension effects.

Clearly, we may not ignore  $\sigma$  or  $B$ , for if either is zero, there would be no interaction between the field and the fluid. Since oscillations are observed for quite small values of  $B$ , we must keep  $\rho$  and  $g$  in the problem to provide a (gravity wave) mechanism for oscillation at low field strength. Hence the relevant parameters are  $\rho, g, \sigma, a, B_0, \mu$ .

With these parameters we form three characteristic velocities:

A diffusion speed

$$V_D = \frac{1}{\mu\sigma a} ;$$

The velocity of Alfven waves

$$V_A = \frac{B_0}{\sqrt{\mu\rho}} ;$$

and a gravity speed

$$V_g = \sqrt{ga}$$

We define two nondimensional parameters:

The "magnetic Reynolds number"

$$Rm = \frac{V_G}{V_d} = \mu_0 \sigma a \sqrt{ga} \quad ;$$

and the Alfven number

$$\alpha = \frac{V_A}{V_G} = \frac{Bo}{\sqrt{\mu_0 \rho g a}}$$

For the solenoid filled with mercury described above

$$Rm = .08 \quad ;$$

and in the experiments performed,

$$4 < \alpha < 7.$$

Hence we consider the axisymmetric motion of the free surface of a conducting incompressible fluid, in a deep cylindrical tank, under the influence of a changing magnetic field.

Since the boundary conditions at the free surface are nonlinear, the only way to make progress in deep water problems is to linearize (about  $Bo$ ), considering the ratio of maximum wave amplitude  $\zeta_0$  to wave length,  $\lambda$ , to be small. This results in the classical gravity wave theory when either  $\alpha$  or  $Rm$  is zero.

However, even the linearized problem for arbitrary  $\alpha$ ,  $Rm$ , appears extremely difficult with the geometry of the cylindrical tank. This arises due to the complexity of the magnetic boundary conditions. To see this, choose cylindrical coordinates  $(r, \theta, z)$  with  $\vec{1}_z$  pointing upwards. To lowest order, the free surface is at  $z = 0$ ,  $0 < r < a$ . We idealize the solenoid to a current sheet in the  $\vec{1}_\theta$  direction at  $r = a$ ;

$-\infty < z < +\infty$ . We consider a current sheet of strength  $I \frac{\text{amps}}{\text{meter}}$ , which changes by a small amount. Now, at the boundaries of fluid and the solenoid, the tangential jump in magnetic field is equal to the current sheet at the boundary, and  $B_{\text{normal}}$  is continuous. There is no current sheet on the free surface when the fluid has finite conductivity. Now consider the fluid replaced by a solid conductor. With changing  $I$ , some of the magnetic field will be pushed outside the solenoid due to the current in the solid conductor. Hence only at  $z = +\infty$  do we know the value of  $\vec{B}$ , i. e.,  $B_z(r = a+) = 0$ ;  $B_r(r = a) = 0$ . Hence the value of the magnetic field at the boundaries is unknown for  $z$  finite, and the magnetic boundary conditions are functional relations on the magnetic field in the three regions  $r > a$ ,  $-\infty < z < \infty$ ;  $0 < r < a$ ,  $-\infty < z < 0$  and  $0 < r < a$ ,  $0 < z < \infty$ . This poses a formidable problem, which for given  $I(t)$  has no simple analytic solutions. Finally, when the fluid motion is considered coupled to the magnetic field, it appears hopeless to try to get solutions without numerical computation.

To understand the effects of finite conductivity and field strength, we must seek a simpler problem that avoids the complexity associated with the walls of the solenoid. From the results of such a problem, we should be able to construct an approximate theory based upon the fact that  $Rm$  in the experiments and preliminary observations is small. The problem we choose to solve for finite conductivity and field strength is that of the response to a one dimensional pressure pulse given by

$$P(x, \zeta, t) = p_0 \delta(x) \delta(t)$$



as the disturbance propagates across an infinitely deep and wide "ocean" of conducting fluid. The vertical direction is  $z$ ;  $\zeta = z$  is the equation of the surface.

We solve this problem for fixed  $\alpha$ ,  $R_m$  and then for  $R_m \rightarrow 0$ ,  $\alpha^2 R_m \sim 1$ , which turns out to be the distinguished limit process which applies to the experiment. Finally, we solve the solenoid problem in this limiting case. Details of these solutions, and the experiment, are given in appendices. Here we shall give a summary of the principal results of these theories, and the experiment.

First it is convenient to review two relevant problems in classical gravity wave theory.

## II. Deep Water Gravity Wave Theory

This section is a brief review of two problems in deep water gravity wave theory which are relevant to the subsequent magnetohydrodynamic theory. We first consider the disturbance caused by a one dimensional pressure pulse on an infinite ocean. The disturbance is given by

$$P(x, \zeta, t) = P_0 \delta(x) \delta(t) \quad 2.1$$

where  $P$  is the pressure, the upward vertical direction is  $\hat{T}_z$ , and the equation of the surface is  $\zeta = z$ .  $\delta(x)$ ,  $\delta(t)$  are Dirac delta functions defined by

$$\int_{-\infty}^{\infty} \delta(x) dx = 1 ; \int_{-\infty}^{\infty} f(x) \delta(x) dx = f(0)$$

Hence  $\delta(x) \delta(t)$  has dimensions  $\frac{1}{\text{length} \times \text{time}}$ . Thus we may find a characteristic length for the problem,  $\lambda_0$ , given by

$$\lambda_0 = \left[ \frac{1}{g} \left( \frac{P_0}{\rho} \right)^2 \right]^{1/5} \quad 2.2$$

Clearly, from its construction,  $\lambda_0$  can play no fundamental role in the solution. We introduce  $\lambda_0$  in this and following problems as a convenience, permitting use of the solutions of these problems in the construction of the solution to the solenoid problem, where there is a true length, the radius of the solenoid. We nondimensionalize using  $\lambda_0$ ,  $\rho$ ,  $g$ . Then the linearized equations of motion for an inviscid incompressible flow have a harmonic velocity potential  $\phi$ :

$$\frac{\partial^2 \phi}{\partial x^2} + \frac{\partial^2 \phi}{\partial z^2} = 0 \quad 2.3$$

The linearized boundary conditions at the free surface are, at  $z = 0$ :

$$\frac{\partial \phi}{\partial t} - \zeta = \delta(x) \delta(t) \quad 2.4$$

and

$$-\frac{\partial \phi}{\partial z} = \frac{\partial \zeta}{\partial t} \quad 2.5$$

As  $z \rightarrow -\infty$ ;  $\phi \rightarrow 0$ , because the disturbance due to the surface motion dies out far below the surface. Equations 2.3, 2.4 and 2.5 form a correctly posed problem in terms of the nondimensional velocity potential  $\phi$ , and surface shape  $\zeta$ .

In terms of inverse Fourier and Laplace transforms, the solution for  $\zeta$  may be written as

$$\zeta = \lim_{z \uparrow 0} \left\{ -\frac{1}{4\pi^2 i} \int_{-\infty}^{\infty} e^{ikx} dk e^{|k|z} \int_{-i\infty}^{i\infty} \frac{e^{st} ds |k|}{s^2 + |k|} \right\} \quad 2.6$$

Hence we have reduced the problem to that of finding the poles of

$$\frac{1}{H(s, k)} = \frac{|k|}{s^2 + |k|} \quad 2.7$$

and evaluating an integral over all wave numbers  $k$ . When approximations to  $\zeta$  are made by the methods of steepest descent or stationary phase, the factor  $e^{|k|z}$  in equation 2.6 plays no

role, hence for convenience we write  $\zeta$  without the limit sign and set  $z = 0$  in the integrand, keeping in mind that the resulting divergent integral is only a convenient representation of the convergent integral of equation 2.6.

Keeping these remarks in mind, we find that contour integration gives

$$\zeta = -\frac{1}{2\pi} \int_0^{\infty} \sqrt{k} \cos kx \cos(\sqrt{k}t - \frac{\pi}{2}) dk \quad 2.8$$

We approximate equation 2.8 for large  $t$  by applying the method of stationary phase. The point of stationary phase is given by

$$k_0 = \frac{1}{4} \left( \frac{t}{x} \right)^2 \quad 2.9$$

and we find

$$\zeta \sim -\frac{1}{4\sqrt{2\pi}} \frac{t^2}{x^{5/2}} \sin(k_0 x - \frac{\pi}{4}) \quad 2.10$$

as

$$t^2/x \rightarrow \infty ; x \neq 0.$$

We see that for  $t/x$  small, we get a long wavelength disturbance; for  $t/x$  large, a short wavelength disturbance. Considering the leading edge of the wave to be near the  $x$  axis on an  $(x, t)$  diagram, and the trailing edge to be near the  $t$  axis, we say that the leading edge is composed of long waves, and the trailing edge of the wave is composed of short waves.

We understand this result by noting that the initial disturbance  $\delta(x)\delta(t)$  may be viewed as a source of all frequencies and wavelengths,

and that the phase velocity of a gravity wave, of wavelength  $\lambda$ , in deep water, is given by

$$V_P \sim \sqrt{\lambda} \quad 2.11$$

Hence long waves travel faster than short waves, and the leading edge is composed of long waves. (For a complete discussion of this result see Stoker, Ref. 1, p. 167)

Now, we remark that in a more complicated problem,  $H(s, k)$  (Eq. 2.7) may not have simple algebraic zeros. If we find approximate zeros of  $H(s, k)$  for  $k \ll 1$ , and then apply the method of stationary phase, we would expect the results to be valid in some sense only when  $k_0 \ll 1$ .

The second problem is to find the resulting motion, when the free surface of a vertical deep cylindrical tank of radius  $a$  is released from an initial shape  $\zeta(r, 0) = f(r)$ . Again we consider an inviscid, incompressible fluid. We choose  $\vec{1}_z$  to be along the axis of the tank, and consider the equation of the surface to be

$$z = z_0 + \zeta(r, t) \quad 2.12$$

where  $z_0$  is the level of the undisturbed surface:

$$\int_0^a r(\zeta(r, 0) + z_0) dr = 0, \quad 2.13$$

and  $r$  is the cylindrical radius. We nondimensionalize as before, replacing  $\lambda_0$  by  $a$ . Then the equations and boundary conditions for  $\phi$  and  $\zeta$  are

$$\frac{1}{r} \frac{\partial}{\partial r} r \frac{\partial \phi}{\partial r} + \frac{\partial^2 \phi}{\partial z^2} = 0 \quad 2.14$$

Since no fluid flows through the wall

$$\left. \frac{\partial \phi}{\partial r} \right|_{r=1} = 0 \quad 2.15$$

and at the free surface, we find, as before, for  $t > 0$

$$\frac{\partial^2 \phi}{\partial t^2} + \frac{\partial \phi}{\partial z} = 0 \quad 2.16$$

$$-\frac{\partial \phi}{\partial z} = \frac{\partial \zeta}{\partial t} \quad 2.17$$

$$\text{As } z \rightarrow \infty, \phi \rightarrow 0. \quad 2.18$$

The solution to this problem is obtained by separation of variables. We find that

$$h(r, t) = \sum A_n \cos \sqrt{k_n} t J_0(k_n r) \quad 2.19$$

where  $k_n$  is the  $n$ th zero of

$$J_1(k_n) = 0 \quad 2.20$$

and the  $A_m$  are given by

$$A_m = \frac{2}{J_0^2(k_m)} \int_0^1 t f(t) J_0(k_m t) dt \quad 2.21$$

Such an expansion in Bessel functions,  $J_0(k_n r)$ , is called a Dini series. (See Watson, Ref. 2, p. 576 ff).

In the magnetohydrodynamic problem of the disturbance caused by a pressure pulse on an infinite ocean of conducting fluid, we shall find that equation 2.10 is an approximation to  $\zeta$  at the leading and trailing edges of the disturbance. In the problem with a solenoid half filled with mercury, the solution comes out in a Dini series of exactly the same form in  $r$  variation as in equation 2.19.

### III. Theory of Magnetohydrodynamic Deep Water Waves

In this section we shall discuss the results of the pressure pulse problem described in Section II for the case of finite conductivity and a vertical magnetic field  $B_0$ . Details of the solution are given in Appendix I.

As in Section II, we consider a linearized problem, with the small parameters being  $\zeta_0/\lambda = \frac{\text{maximum surface deflection}}{\text{wave length}}$ . In particular, we consider the magnetic field to be given by

$$\frac{\vec{B}}{B_0} = \vec{1}_z + \vec{b}, \quad \vec{b} \sim O\left(\frac{\zeta_0}{\lambda}\right) \quad 3.1$$

where  $\vec{1}_z$  is the vertical direction.

As in Section II, we nondimensionalize with a length  $\lambda_0$  derived from the initial conditions. We assume that the non-dimensional velocity  $\vec{v}$ , electric field  $\vec{e}$ , current density  $\vec{j}$  and magnetic field perturbation  $\vec{B}$ , are all of the same order of magnitude. We nondimensionalize with  $B_0, \lambda_0, \rho, g, \mu, \sigma$  in such a way that Maxwell's equations become

$$-\frac{\partial \vec{B}}{\partial t} = \text{curl } \vec{e} \quad 3.2$$

$$\vec{j} = \vec{e} + \vec{v} \times \vec{1}_z \quad 3.3$$

$$\text{curl } \vec{B} = Rm \vec{j} \quad 3.4$$

$$\text{div } \vec{b} = 0 \quad 3.5$$



where, as mentioned in Section I, we have ignored the displacement current.

Now, using equations 3.2, 3.3 and 3.4, we eliminate  $\vec{e}$  and  $\vec{j}$  to form the induction equation in terms of  $\vec{v}$  and  $\vec{b}$ . It is

$$\frac{\partial \vec{b}}{\partial t} = \frac{\nabla^2 \vec{b}}{Rm} + \frac{\partial \vec{v}}{\partial z} \quad 3.6$$

where  $Rm = \mu \sigma \lambda_o \sqrt{g \lambda_o}$  in equations 3.4, 3.6.

The linearized momentum equation is, in these non-dimensional variables,

$$\frac{\partial \vec{v}}{\partial t} = -\vec{v} p + \alpha^2 Rm \vec{j} \times \vec{1}_z - \vec{1}_z \quad 3.7$$

where  $\alpha = \frac{Bo}{\sqrt{\mu \rho g \lambda_o}}$ . The term  $-\vec{1}_z$  is the acceleration due to gravity,  $p$  is the pressure, and  $\alpha^2 Rm(\vec{j} \times \vec{1}_z)$  is the linearized Lorentz force.

The continuity equation

$$\text{div } \vec{v} = 0 \quad 3.8$$

is of course unchanged.

Equations 3.2 through 3.8 are the linearized magnetohydrodynamic equations for an incompressible, inviscid fluid with arbitrary conductivity for  $z < 0$ . For  $z > 0$ , we set  $\vec{j} = \vec{v} = p = 0$  in equations 3.2 through 3.8.

For the present problem, there are four boundary conditions at the free surface. The equation for the free surface is

$$\zeta(x, t) - z = 0 \quad 3.9$$

The first boundary condition states that for  $t \neq 0$ ,  $x = 0$ , the pressure at the surface is zero. Hence

$$p(x, \zeta, t) = \delta(x) \delta(t) \quad 3.10$$

where  $\delta(x)\delta(t)$  is the pressure pulse.

The second boundary condition is that no fluid flows through the free surface. When linearized, this condition becomes

$$\frac{\partial \zeta}{\partial t} = v_z(x, 0, t) \quad 3.11$$

where  $v_z$  is the velocity in the  $\vec{I}_z$  (vertical) direction. Equations 3.10 and 3.11 are exactly the same boundary conditions as equations 2.4 and 2.5, except that here the fluid motion is rotational, and hence there is no longer a velocity potential.

The last two boundary conditions at the surface are on the magnetic field. The third is that from equation 3.5, the normal component of  $\vec{b}$  is continuous across the surface. When linearized, this becomes

$$b_z(x, 0-, t) = b_z(x, 0+, t) \quad 3.12$$

where  $b_z$  is the vertical component of  $\vec{b}$  and

$$b_z(x, 0-, t) = \lim_{z \uparrow 0} b_z(x, z, t)$$

The fourth surface boundary condition states that a fluid with finite conductivity cannot support a current sheet. Hence

$$\vec{b}_x(x, 0^-, t) = \vec{b}_x(x, 0^+, t) \quad 3.13$$

Equations 3.9 through 3.13 are the boundary conditions at the surface. To these we must add the fact that all perturbations must die out as  $z$  becomes large. Hence, as  $z \rightarrow +\infty$ ,  $\vec{b} \rightarrow 0$ , and as  $z \rightarrow -\infty$ ,  $\vec{v} \rightarrow 0$ ,  $p + z \rightarrow 0$  and  $\vec{b} \rightarrow 0$ .

The problem is solved by using a Fourier transform on  $x$ , and a Laplace transform on time, and approximating the resulting formulae for the inverse transforms, which are in the form of double integrals over the wave number,  $k$ , and frequency,  $s$ . Due to the fact that the function corresponding to  $H(s, k)$  in Section II is very complicated, we can obtain simple analytic approximations to the solution only at the leading and trailing edges of the surface.

We find that, at the leading and trailing edges of the wave, the simplest approximation to  $\zeta$  is equation 2.10. The nature of such approximations is made explicit in Appendix I and Appendix II; for example, at the trailing edge of the wave, the next approximation to 2.10 is

$$\eta \sim -\frac{1}{4\sqrt{2\pi}} \frac{t^2}{X^{5/2}} e^{-\alpha^2 R_m t} \sin\left(\frac{t^2}{4X} - \frac{\pi}{4}\right) \quad 3.14a$$

as  $t^2/x \rightarrow \infty$ ,  $x \neq 0$ , and  $\frac{t}{x} \rightarrow \infty$ . The analogous correction at the leading edge of the wave is a change in  $k_0$  which results in

a change in phase of  $\zeta$ . That is,

$$\eta(x,t) \sim -\frac{1}{4\sqrt{2}\pi} \frac{t^2}{x^{5/2}} \sin\left\{\frac{t^2}{4x}\left(1 + \frac{1}{8}\alpha^2\left(\frac{t}{x}\right)^2\right) - \frac{\pi}{4}\right\} \quad 3.14b$$

as  $t/x \rightarrow 0$ ;  $t, x \rightarrow \infty$ ;  $t^2/x \rightarrow \infty$ .

We may define a local magnetic Reynolds number,  $\tilde{Rm}$ , based on the local wave number  $k$ , and the local gravity wave phase velocity,  $\sqrt{g/k}$ . Hence  $\tilde{Rm} = \frac{\mu\sigma}{k} \sqrt{g/k}$ . Then at the leading edge of the wave,  $\tilde{Rm} \rightarrow \infty$ , and the trailing edge of the wave,  $\tilde{Rm} \rightarrow 0$ . Thus the leading edge of the wave is a region of high conductivity effects, and the trailing edge of the wave a region of low conductivity effects.

This means that a limit  $\tilde{Rm} \rightarrow \infty$  is uniformly valid only when  $k \rightarrow 0$ , and that a limit of  $\tilde{Rm} \rightarrow 0$  is uniformly valid only when  $k \rightarrow \infty$ ; for, whatever the conductivity, the region at the trailing edge of the wave is one where  $k \rightarrow \infty$ , and the region at the leading edge of the wave, one where  $k \rightarrow 0$ . Finally, these limits on  $\tilde{Rm}$  correctly model the leading and trailing edges of the wave.

The reason that we nondimensionalized with a somewhat peculiar length  $\lambda_0$  derived from initial conditions is that only with this nondimensionalization does the connection between wave number and low and high conductivity limits become clear.

However, the problem has much more structure than indicated above. This is due to the fact that the surface is an emitter of Alfvén waves. To see this, we take the curl of equations 3.6 and 3.7. We get

$$\frac{\partial \bar{\omega}}{\partial t} = \alpha^2 R_m \frac{\partial \bar{j}}{\partial z} \quad 3.15$$

$$R_m \frac{\partial \bar{j}}{\partial t} = \nabla^2 \bar{j} + \frac{\partial \bar{\omega}}{\partial z} \quad 3.16$$

where  $\bar{\omega} = \text{curl } \bar{v}$  is the vorticity. Eliminating  $\bar{\omega}$ , we find that

$$\frac{\partial^2 \bar{j}}{\partial t^2} - \alpha^2 \frac{\partial^2 \bar{j}}{\partial z^2} = \frac{1}{R_m} \frac{\partial}{\partial t} \nabla^2 \bar{j} \quad 3.17$$

which is the equation for Alfvén waves propagating along the unperturbed field lines  $\bar{T}_z$ , with speed  $\alpha$ . Equations 3.15 and 3.16 describe the production and propagation of current and vorticity.

That vorticity is produced is easy to see, for although the fluid motion is irrotational initially, it can not remain so since the Lorentz force in the momentum equation is non-conservative. Hence any surface motion must produce vorticity, and hence currents, which then propagate according to equations 3.15 and 3.16. We find that the vorticity may be considered as being produced at the surface (see Appendix I).

Now the vorticity produced at the surface should have the same local wave number, say  $k$ , as the surface deflection at the same point. From equation 3.15, the current produced must have the same wave number as the vorticity.

To find the structure of the Alfvén wave emission, we consider a given initial current  $j(x, 0, t)$  and use equation 3.17 to find out how it propagates. At a point where the surface has a wave number  $k$ , the initial current is of the form

$$j(x, 0, t) \sim e^{ikx} f(t) \quad 3.18$$

At the leading edge of the wave,  $k \rightarrow 0$ . Hence  $\bar{j}$  is nearly independent of  $x$ . But if  $j$  is independent of  $x$ , equation 3.17 becomes formally identical to the equation for a sound wave in viscous fluid. Hence we expect a plane wave front traveling with speed  $\alpha$ , diffusing isotropically as  $\alpha^2 Rm$ . The detailed computation shows this to be the case. At the surface,  $j$  has the same local wave number as the surface deflection, when  $k \rightarrow 0$ .

At the trailing edge of the wave,  $k \rightarrow \infty$ ,  $j(x, 0, t)$  is a rapidly oscillating function of  $x$ . We find that diffusion of current is the dominant feature, and no propagation occurs. Again, as  $k \rightarrow \infty$ , the wave numbers of the surface deflection and current  $j(x, 0, t)$  are the same.

Finally, we seek limit processes on the conductivity,  $Rm$ , and Alfvén speed,  $\alpha$ , which will correctly describe both the surface deflections and Alfvén wave structure at high and low wave numbers. First we consider the case of low wave number,  $k \rightarrow 0$ . Then we know from the discussion above, that if  $\alpha$  and  $\alpha^2 Rm$  are held fixed, we shall describe correctly the Alfvén wave propagation. But to describe the surface deflections, we must require  $Rm \rightarrow \infty$ . This is inconsistent with holding both  $\alpha$  and  $\alpha^2 Rm$  fixed. We conclude that such a limit does not exist for  $k \rightarrow 0$ . We find that in a limit where  $Rm \rightarrow \infty$ ,  $\alpha$  fixed, we must apply radiation boundary conditions at  $z = -\infty$ , in contrast with the problem formulated for  $Rm$  finite.

Next, we turn to the high wave number case. To describe the surface deflection, we must require  $Rm \rightarrow 0$ . There is no Alfvén wave propagation, only diffusion of currents. We find that  $\alpha^2 Rm$  is again

the parameter governing diffusion, as  $k \rightarrow \infty$ . Hence we consider the limit  $Rm \rightarrow 0$ ,  $\alpha^2 Rm \sim 1$ . This is the physically distinguished limit of the problem, for it correctly describes both the Alfvén wave structure and surface deflection as  $k \rightarrow \infty$ .

Finally, since the surface deflection for large  $k$  is approximated by gravity waves, we may estimate the lowest wave numbers occurring in the solenoid problem using the results of the second example in Section II. There, the lowest wave number was given by  $J_1(k_1) = 0$ ;  $k_1 = 3.84$ . Since  $Rm = .08$  for the solenoid problem, and for the experiment,  $1 < \alpha^2 Rm < 5$ , we expect that the limit process  $\alpha^2 Rm \sim 1$ ,  $Rm \rightarrow 0$  contains the correct description of all effects occurring in the solenoid problem, and hence is the correct linearized description of the problem.

The assumption that the mercury is infinitely deep is valid, for the bottom of the mercury tank can have little influence on the free surface when the Alfvén wave structure is diffusive.

#### IV. Theory of the Limiting Case $Rm \rightarrow 0$ , $\alpha^2 Rm \sim 1$

To study the properties of the distinguished limit found in Section III, we must find the response of an infinite ocean of conducting fluid to a pressure pulse. Details of the calculation are given in Appendix II.

Under the limit process, we find the following equations for the magnetic field

$$\text{curl } \vec{b} = 0 \quad 4.1$$

$$\text{div } \vec{b} = 0 \quad 4.2$$

where we are using the same nondimensional variables as Section III. Now equations 4.1 and 4.2 are valid both for  $z < 0$  and  $z > 0$ . Further, at the surface,  $\vec{b}$  is continuous and, as  $|z| \rightarrow \infty$ ,  $\vec{b} \rightarrow 0$ . Hence we conclude

$$\vec{b} = 0 \text{ everywhere} \quad 4.3$$

Hence

$$\vec{e} = 0 \quad 4.4$$

and

$$\vec{j} = \vec{v} \times \vec{I}_z \quad 4.5$$

Thus, although the induced electric field  $\vec{v} \times \vec{B}$  is of order one in the limit, the conductivity is so low that the currents produced do not affect the magnetic field.

The momentum and continuity equations are unchanged:



$$\frac{\partial \bar{V}}{\partial t} = -\nabla p + \alpha^2 R_m (\bar{V} \times \bar{I}_z) \times \bar{I}_z - \bar{I}_z \quad 4.6$$

$$\operatorname{div} \bar{V} = 0 \quad 4.7$$

Eliminating  $\bar{V} = (v_x, v_z)$  from equations 4.6 and 4.7 results in the following fundamental equation for the pressure:

$$\frac{\partial}{\partial t} \nabla^2 p + \alpha^2 R_m \frac{\partial^2 p}{\partial z^2} = 0 \quad 4.8$$

The equation expresses the damping effect of the Lorentz force

$$\alpha^2 R_m (\bar{V} \times \bar{I}_z) \times \bar{I}_z = -\alpha^2 R_m V_x \bar{I}_x$$

in the momentum equation.

The boundary conditions on  $p$ ,  $\bar{V}$  are exactly those of Section III. Expressing them in terms of  $p$ , we have, for a surface shape

$$\zeta(x, t) - z = 0 \quad 4.9$$

the surface boundary conditions

$$p(x, \zeta, t) = \delta(x) \delta(t) \quad 4.10$$

and

$$\frac{\partial^2 \zeta}{\partial t^2} = -\frac{\partial p(x, \zeta, t)}{\partial z} - 1 \quad 4.11$$

As  $z \rightarrow -\infty$ ,  $p + z \rightarrow 0$ , for the surface disturbances die out at  $z = -\infty$ .

Now equation 4.8 with boundary conditions consisting of equations 4.9, 4.10 and 4.11 form a properly posed initial value

problem. We find the solution for  $\zeta(x, t)$  to be, in terms of inverse Fourier and Laplace transforms

$$h(x, t) = \lim_{z \rightarrow 0} \left\{ -\frac{1}{4\pi^2 i} \int_{-\infty}^{\infty} e^{ikx} dk \int_{-i\infty}^{i\infty} \frac{e^{st} e^{2k\sqrt{\frac{s}{R+s}}}}{1 + \frac{s^2}{|k|} \sqrt{\frac{R+s}{s}}} ds \right\} \quad 4.12$$

Keeping in mind that we will approximate  $\zeta(x, t)$  for large  $(x, t)$  as in Section II, we replace equation 4.12 by the divergent integral

$$h(x, t) = -\frac{1}{4\pi^2 i} \int_{-\infty}^{\infty} e^{ikx} dk \int_{-i\infty}^{i\infty} \frac{e^{st} ds}{1 + \frac{s^2}{|k|} \sqrt{\frac{R+s}{s}}} \quad 4.13$$

where  $R$  is the parameter of the limit process

$$R = \alpha^2 R_m \quad 4.14$$

Now inspection of equation 4.13 reveals that we should introduce new coordinates

$$\begin{aligned} x^* &= R^2 x \\ t^* &= Rt \\ s^* &= s/R \\ k^* &= k/R^2 \end{aligned} \quad 4.15$$

$$R^3 \zeta^*(x^*, t^*) = \zeta(x, t)$$

which eliminate  $R$  from the problem. In this way, we find two different approximations for  $\zeta^*(x^*, t^*)$  at the leading edge of the wave,  $k^* \rightarrow 0$ , and at the trailing edge of the wave,  $k^* \rightarrow \infty$ . Details are given in Appendix II.

## V. Linearized Theory of the Solenoid Problem

In this section we discuss the linearized theory of the solenoid problem for the limiting case  $Rm \rightarrow 0$ ,  $\alpha^2 Rm \sim 1$ . As in Section IV, we shall write the parameter of the limit processes as  $R = \alpha^2 Rm$ .

We consider an infinitely long vertical solenoid half filled with mercury. We ask, "What is the response of the free surface, when the current in the solenoid undergoes a small change?" We begin by considering the equations for the magnetic field. For the details see Appendix III.

Let the undisturbed free surface be given by  $z = 0$ ,  $0 < r < 1$ , where  $r$  is the radial distance and  $\vec{I}_z$  is parallel to the axis of the solenoid and positive upward. We assume the motion to be axisymmetric,  $\frac{\partial}{\partial \theta} = 0$ , and nondimensionalize, as in Section II, with  $\rho$ ,  $g$ , and  $a$ , the inner radius of the solenoid.

The equations for the magnetic field, in the limit become

$$\operatorname{div} \vec{b} = 0 \quad 5.1$$

$$\operatorname{curl} \vec{b} = 0 \quad 5.2$$

both for  $z \lesssim 0$ . Far above, and far below the free surface, the magnetic field is given by

$$\frac{\vec{B}}{B_0} = \vec{I}_z + b_z(t) \quad 5.3$$

where  $b_z(t)$  is the field due to the small change in solenoid current. Since  $\vec{b}$  is continuous at  $z = 0$ , we conclude that

$$\vec{b} = b_z(t) \vec{I}_z \quad \text{for all } z, 0 < r < 1 \quad 5.4$$

Clearly,  $\vec{b} = 0$  for  $r > 1$ .

Thus we see the essential simplification that occurs in the limit is that the magnetic field lines are straight.

From equation 5.4, we compute

$$-\frac{db_z}{dt} = \vec{I}_z \cdot \text{curl } \vec{e} = -\frac{1}{R} \frac{\partial}{\partial R} (R e_\theta) \quad 5.5$$

since we have assumed axial symmetry. Thus we find that the nondimensional current  $\vec{j}$  is:

$$\vec{j} = \frac{db_z}{dt} \frac{R^2}{2} \vec{I}_\theta + \vec{v} \times \vec{I}_z \quad 5.6$$

Hence the momentum equation becomes

$$\frac{\partial \vec{v}}{\partial t} = -\nabla p + R \left( \frac{db_z}{dt} \frac{R^2}{2} \vec{I}_\theta + \vec{v} \times \vec{I}_z \right) \times \vec{I}_z - \vec{I}_z \quad 5.7$$

The continuity equation is unchanged.

$$\text{div } \vec{v} = 0 \quad 5.8$$

Upon eliminating  $\vec{v}$  from equations 5.7 and 5.8, we find the same equation for  $p$  as in Section IV except that now it has a right hand side which is the forcing function caused by the changing solenoid current.

$$\frac{\partial \nabla^2 p}{\partial t} + R \frac{\partial^2 p}{\partial z^2} = -R \frac{d^2 b_z}{dt^2} \quad 5.9$$

The boundary conditions at the free surface are

$$p(x, \zeta, t) = 0 \quad 5.10$$

$$\frac{\partial^2 \zeta}{\partial t^2} = \frac{\partial p}{\partial z} - 1 \quad 5.11$$

At the wall,  $v_r = 0$ . In terms of pressure this means

$$\frac{\partial p}{\partial r}(r=1, z, t) = 0 \quad 5.12$$

Far from the free surface, the velocity must die out. As  $z \rightarrow -\infty$ , we use the momentum equations with  $v \rightarrow 0$ , to find

$$p + z \rightarrow f(r) \quad 5.13$$

The solution of the mathematical problem posed by equation 5.9 with boundary conditions consisting of equations 5.10 through 5.13 is solved by assuming a Dini series expansion in  $J_0(k_m r)$  and taking the Laplace transform of time.

As in Section IV, we define new variables

$$k_m^* = k_m / R^2 \quad 5.14$$

$$t^* = R t$$

Then the solution for  $\zeta(r, t)$  may be written as a product of a Dini series times convolution integrals.

$$h(r, t) = R \sum_m l_m(t^*, k_m^*, \frac{db_z}{dt^*}) \frac{J_0(k_m R)}{2 k_m^2} \quad 5.15$$

where

$$J_1(k_m) = 0 \quad 5.16$$

and, for  $k_m^* \gg 1$ ,

$$l_m(t^*, k_m^*, \frac{db_z}{dt^*}) = \int_0^{t^*} \frac{db_z(t^*-s)}{dt^*} \frac{e^{-\frac{1}{4}s} \cos(\sqrt{k_m^* - \frac{3}{16}}s - \frac{\pi}{2})}{\sqrt{k_m^* - \frac{3}{16}}} ds \quad 5.17$$

and for  $k_m^* \ll 1$

$$l_m(t^*, k_m^*, \frac{db_z}{dt^*}) = \int_0^{t^*} \frac{db_z(t^*-s)}{dt^*} \frac{e^{-\frac{1}{2}k_m^* \frac{2}{3}s} \cos(\sqrt{\frac{3}{2}}k_m^*s - \frac{\pi}{3})}{\frac{2}{3}k_m^* \frac{1}{3}} ds \quad 5.18$$

The  $l_m$  are analogous to the approximations for the leading and trailing edge of the wave in Section IV.

Inspection of equations 5.16 and 5.17 shows that as  $\frac{db_z}{dt}$  excites the various damped modes of the system, we get damped oscillations of the free surface.

## VI. Experiments

With a vertical solenoid half filled with mercury, experiments were performed to measure the surface deflections due to a changing current in the solenoid. The experiments were performed at GALCIT in the magneto-fluid mechanic facility (see Ref. 3). The surface deflection was measured by recording the varying resistance of carbon rods grounded in the mercury, as the surface oscillated. This was done simultaneously at four different radii, producing a recording of the instantaneous surface shape. To induce the surface oscillations, the solenoid was switched off or on. Details of the experiment are presented in Appendix IV.

When the magnet was switched off, the field changed as

$$B = B_0 e^{-R/L t} \quad 6.1$$

The field changed as

$$B = B_0 (1 - e^{-\lambda t}) \quad 6.2$$

when the field was switched on. The field inside the solenoid was not measurably affected by the presence of the mercury, indicating that the limit  $Rm \rightarrow 0$  is correct.

The oscillations observed reached a nondimensional amplitude in the center of the tank of

$$\zeta_{\max} = .7 \quad 6.3$$

i. e. , a 5 cm. deflection in a tank of radius 7 cm.

Under these conditions, application of a linearized theory would appear dubious, but the experimental results qualitatively check all the features of the theory. See Appendix IV for graphical comparisons of the theory and experiment.



## VII. Discussion of Previous Work

This section consists of a brief review of several types of magnetohydrodynamic surface waves, and some remarks on the shallow water theory analogous to the deep water theory presented above.

### a) General

The theory of water waves is a classical subject, with a large literature. One recent book is that of Stoker (Ref. 1). It contains a modern treatment of the pressure impulse problem (see Sec. II), and a discussion of shallow water theory which Fraenkel (Refs. 6, 7) uses (see below), as well as many other topics.

As to magnetohydrodynamic surface waves, a survey of the literature reveals that there are many types of magnetohydrodynamic interactions. All authors mentioned below consider an incompressible, inviscid fluid.

For example, Solov'ev (Ref. 4) considers a fluid (plasma) with infinite conductivity. Outside the fluid, and parallel to its surface is a magnetic field. The magnetic field does not penetrate the fluid. Initially, the surface of the fluid is undisturbed, and the magnetic pressure is constant on the surface. However, a surface deflection causes a variation in the magnetic pressure at the surface of the fluid, which under appropriate circumstances can cause the disturbance to propagate. Solov'ev finds the circumstances under which solitary waves can exist, for example. He ignores the effects of gravity.

Another class of electro- and magneto-hydrodynamic surface waves is considered by Melcher (Ref. 5). Consider a heavy fluid with

zero conductivity but high dielectric constant. If a strong electric field is applied to the fluid, the free surface of the fluid will be stressed by the Maxwell stress due to the jump in dielectric constant. In studying this problem, Melcher finds an electric analog to the Alfvén speed,  $\frac{Bo}{\sqrt{\mu\rho}}$ .

#### b) Shallow Water Theory

Consider an inviscid, incompressible conducting fluid, that is contained in a shallow disk of depth  $H_0$ , and horizontal dimension  $L$ . We prescribe a vertical magnetic field  $Bo$ , and ask as to the nature of the waves produced under the action of gravity, and the effects of  $Bo$ . As in our previous work, it is convenient to form an Alfvén number and magnetic Reynolds number, based upon a characteristic length and gravity speed. Thus, here we have

$$Rm = \mu\sigma L \sqrt{g H_0} \quad 7.1$$

$$\alpha = \frac{Bo}{\sqrt{\mu\rho g H_0}} \quad 7.2$$

We derive the equations from a limit process on  $\epsilon = H_0/L \rightarrow 0$ . The magnetohydrodynamic shallow water theory is due to Fraenkel (Refs. 6, 7) and Lundquist (Ref. 8). Fraenkel considers the case

$$\begin{aligned} Rm &\rightarrow 0 \\ \alpha^2 Rm &\sim 1 \quad \text{as } \epsilon \rightarrow 0 \end{aligned} \quad 7.3$$

As with our work, he finds this limit to be the one applicable for experiments in mercury. In close analogy with our results, he

finds that the effect of  $\alpha^2 Rm$  is to provide a damping term linear in the horizontal velocity, and, in the linearized theory, that disturbances propagate with the gravity velocity,  $\sqrt{gH_0}$ . This theory is fairly simple, due principally to the fact that the gravity wave theory, which Fraenkel's theory reduces to as  $\alpha^2 Rm \rightarrow 0$ , does not contain dispersion in its linearized form. In analogy with deep water theory, we expect the limit  $\alpha^2 Rm \sim 1$ ,  $Rm \rightarrow 0$  to be not uniformly valid for small wave numbers, but this has not been shown.

Lundquist (Ref. 8) has studied the shallow water theory in the case

$$Rm \rightarrow \infty, \alpha \text{ fixed as } \epsilon \rightarrow 0 \quad 7.4$$

He finds that the wave velocity becomes

$$c = \sqrt{\frac{B_0^2}{\mu \rho} + g H_0} \quad 7.5$$

the combined speed, familiar from the analogous compressible case. Again, the equations are quite simple due to the lack of dispersion or damping. Lundquist shows that his theory is valid only for small wave numbers.

We speculate that the increase in speed from  $\sqrt{gH_0}$  to  $\sqrt{\frac{B_0^2}{\mu \rho} + gH_0}$  as  $Rm$  increases, may be alternately expressed as a limit on the wave number, and as such, may be understood by solving the linearized problem for a finite depth  $H_0$ , and finite  $\alpha$ ,  $Rm$ , and then examining the solution as  $H_0/L \rightarrow 0$ . Hence, in contrast to the classical theory, the shallow water magnetohydrodynamic theory is dispersive.

Presumably, the finite depth causes a multiple reflection of the long Alfvén waves emitted from the surface, which causes the speed of propagation to increase.

## APPENDIX I

## Theory of Magnetohydrodynamic Surface Waves

This appendix is a study of a deep water theory of magnetohydrodynamic gravity waves. Such a theory would describe the motion of a liquid metal contained in the presence of an externally applied vertical magnetic field.

The basic assumptions of the theory are: 1) the depth,  $d$ , of the fluid is large compared to any wave length  $\lambda$  considered; i. e.,  $\frac{\lambda}{d} \rightarrow 0$ . 2) the maximum wave amplitude  $\zeta_0$  is small compared to  $\lambda$ ; i. e. the equations are linearized with  $\zeta_0/\lambda$  as the small parameter. 3) there is an externally applied vertical magnetic field.

Solutions are obtained for arbitrary conductivity  $\sigma$ , and external field strength  $B_0$ . The fluid is inviscid and incompressible. The magnetic permeability of the fluid is that of free space.

## A. Basic Equations

The linearized equations for a semi-infinite conducting, incompressible inviscid fluid under the action of gravity and an externally applied magnetic field are, for the case of two dimensional motion:

$$\rho \frac{\partial \vec{v}}{\partial t} = -\nabla p + \frac{B_0}{\mu} \text{curl } \vec{b} \times \vec{1}_z - \rho g \vec{1}_z \quad 1a.1$$

$$\frac{\partial \vec{b}}{\partial t} = \frac{\nabla^2 \vec{b}}{\mu \sigma} + B_0 \frac{\partial \vec{v}}{\partial t} \quad 1a.2$$

$$\nabla \cdot \vec{b} = 0 \quad 1a.3$$

$$\nabla \cdot \vec{v} = 0 \quad 1a-4$$

where  $\rho$  is the fluid density,  $\mu$  is the permeability,  $\sigma$  is the conductivity, and  $g$  is the acceleration due to gravity. The displacement current is neglected.  $\vec{1}_z$  is the vertical direction. The magnetic field is given by

$$\begin{aligned}\vec{B} &= B_0 \vec{1}_z : \vec{b} ; & b \sim 0 (\zeta_0/\lambda) \\ \vec{b} &= b_z \vec{1}_z + b_x \vec{1}_x\end{aligned}\tag{1a-5}$$

The linearized velocity field is

$$\vec{v} = v_x \vec{1}_x + v_z \vec{1}_z \sim 0 (\zeta_0/\lambda)\tag{1a-6}$$

The equations are written in MKSQ units.

At the surface

$$\zeta(x, t) - z = 0 ,\tag{1a-7}$$

the pressure is zero:

$$p(x, \zeta, t) = 0\tag{1a-8}$$

and no fluid flows through the surface:

$$\frac{\partial \zeta}{\partial t} = v_z\tag{1a-9}$$

The normal component of the magnetic field,  $b_n$ , is continuous across the surface. To lowest order this means

$$b_z(x, 0^-, t) = b_z(x, 0^+, t)\tag{1a-10}$$

Finally, a fluid with finite conductivity cannot support a current sheet, hence the tangential component of the magnetic field,  $b_t$  is

continuous at the surface:

$$b_x(x, 0-, t) = b_x(x, 0+, t) \quad 1a-11$$

The notation  $b_x(x, 0-, t)$  is explained in Section III. Equations 1a-7 to 1a-11 are the boundary conditions at the surface on equations 1a-1 to 1a-6.

Above the surface ( $z > 0$ ) we obtain the equations for the magnetic field by setting  $\vec{v} = p = \vec{j} = 0$ .

At  $z = +\infty$ ,  $\vec{b} = 0$ , for the perturbation magnetic field due to the surface motion must die out far above the surface. Far below the surface, all disturbances due to the surface must die out. Hence

$$p + \rho gz \rightarrow 0 ; \vec{v} \rightarrow 0$$

and

$$\vec{b} \rightarrow 0$$

as  $z \rightarrow -\infty$ . This completes the boundary conditions for equations 1a-1 through 1a-6.

Next, we consider the equations for current and vorticity. Let

$$\mu \vec{j} = \text{curl } \vec{b} \quad 1a-12$$

$$\vec{\omega} = \text{curl } \vec{v} \quad 1a-13$$

Clearly, in the case of two dimensional motions considered here,

$$\vec{j} = \vec{I}_y j_y = j \quad 1a-14$$

$$\vec{\omega} = \vec{I}_y \omega_y = \omega \quad 1a-15$$

Taking the curl of equations 1a-1 and 1a-2 gives

$$\frac{\partial j}{\partial t} - \frac{B_0}{\mu} \frac{\partial \omega}{\partial z} = \frac{\nabla^2 j}{\mu\sigma} \quad 1a-16$$

$$\rho \frac{\partial \omega}{\partial t} - B_0 \frac{\partial j}{\partial z} = 0 \quad 1a-17$$

Eliminating the vorticity gives

$$\frac{\partial^2 j}{\partial t^2} - \frac{B_0^2}{\rho\mu} \frac{\partial^2 j}{\partial z^2} = \frac{\partial}{\partial t} \frac{\nabla^2 j}{\mu\sigma} \quad 1a-18$$

This equation describes the propagation of incompressible Alfvén waves, with the usual Alfvén velocity  $\frac{B_0}{\sqrt{\mu\rho}}$ , in the  $\vec{T}_z$  direction.

When  $j$  is independent of  $x$ , equation 1a-18 is exactly analogous to the equations for propagation of sound waves in a viscous medium. However, this analogy is not helpful in general, for sound propagates isotropically, and Alfvén waves propagate along the unperturbed field lines  $\vec{T}_z$ . Further, sound waves are longitudinal and Alfvén waves are transverse.

Due to equation 1a-18 we may evidently expect that any problem concerning the surface motion of a conducting fluid in a magnetic field will have an Alfvén wave structure.

For the initial value problem  $j(x, 0, t) = f(t) \delta(x)$ , the solution of equation 1a-18 may be expressed as

$$j(x, z, t) = \frac{1}{4\pi^2 i} \int_{-i\infty}^{i\infty} \bar{f}(s) e^{st} ds \int_{-\infty}^{\infty} e^{ikx} dk e^{-z \sqrt{\frac{s^2 + sk^2/\mu\sigma}{\alpha^2 + s/\mu\sigma}}} \quad 1a-19$$

where  $\sqrt{\frac{s^2 + sk^2/\mu\sigma}{\alpha^2 + s/\mu\sigma}}$  signifies that the real part of  $\sqrt{\frac{s^2 + sk^2/\mu\sigma}{\alpha^2 + s/\mu\sigma}}$

is  $> 0$  on the path of integration. Since we consider  $k$  real, this requires that the branch cuts of equation 1a-19 run from  $s = 0$ ,



$s = -k^2/\mu\sigma$ , and  $s = \alpha^2/\mu\sigma$  to  $s = -\infty$ . In a problem concerning the surface motion we thus will find branched solutions due to the existence of Alfvén waves.

The most general solution for currents due to vorticity produced at  $z = 0$  is

$$J(x, z, t) = \frac{1}{4\pi^2 c} \int_{-i\infty}^{i\infty} \int_{-\infty}^{\infty} \bar{J}(s, k) e^{ikx} e^{st} e^{z\sqrt{\frac{s^2 + sk^2/\mu\sigma}{\alpha^2 + \frac{s}{\mu\sigma}}} dk ds \quad 1a-20$$

where the branch cuts in the  $s$  plane are as before.

Due to the fact that the Lorentz force in the momentum equation is not in general conservative, we must expect rotational flow fields, and hence production of vorticity.

Hence, substitution of integrals of the form

$$\int_{-\infty}^{\infty} \exp(ikx + \alpha(k)t + \beta(k)z) F(k) dk$$

for an initial value problem would not be correct, unless the contributions of the branch cut integrals are not ignored.

The fact that the motion is assumed two dimensional is not a fundamental restriction; it merely simplifies the resulting integral representation of the solution.

## B. An Initial Value Problem

We consider the response of the fluid and magnetic field to a one dimensional pressure pulse acting on the surface of the fluid.

The boundary condition on the pressure is

$$P(x, \zeta, t) = P_0 \delta(x) \delta(t) \quad 1a-21$$

Since the Dirac delta function is defined by

$$\int_{-\infty}^{\infty} \delta(x) dx = 1 \quad ; \quad \int_{-\infty}^{\infty} f(x) \delta(x) dx = f(0)$$

$\delta(x)$  has dimensions  $\frac{1}{\text{length}}$ . Hence equation 1a-21 defines a length

$$\lambda_0 = \left[ \frac{1}{g} \left( \frac{P_0}{\rho} \right)^2 \right]^{1/5} \quad 1a-21$$

From its construction, it is clear that  $\lambda_0$  can play no fundamental role in the solution.

We denote nondimensional quantities by ( $\tilde{\phantom{x}}$ ), and non-dimensionalize as follows:

$$\zeta = \lambda_0 \tilde{\zeta}$$

$$\vec{v} = \sqrt{g\lambda_0} \tilde{\vec{v}} = \sqrt{g\lambda_0} (\tilde{v}_x \vec{1}_x + \tilde{v}_z \vec{1}_z)$$

$$P = \rho g \lambda_0 \tilde{p}$$

$$\vec{B} = B_0 (\vec{1}_z + \vec{b}) = B_0 ((b_z + 1) \vec{1}_z + b_x \vec{1}_x)$$

$$(x, z, t) = (\lambda_0 \tilde{x}, \lambda_0 \tilde{z}, \sqrt{\frac{\lambda_0}{g}} \tilde{t})$$

This nondimensionalization introduces the parameter

$$\alpha = \frac{Bo}{\sqrt{\mu \rho g \lambda_0}} \quad 1a-23$$

the Alfvén number, into the momentum equation; and the magnetic Reynolds number

$$Rm = \mu \sigma \lambda_0 \sqrt{g \lambda_0} \quad 1a-24$$

in the induction equation. The nondimensional equations are, dropping the  $(\sim)$ 's:

$$\frac{\partial \vec{v}}{\partial t} = -\nabla p + \alpha^2 \text{curl } \vec{b} \times \vec{I}_z - \vec{I}_z \quad 1a-25$$

$$\frac{\partial \vec{b}}{\partial t} = \frac{\nabla^2 \vec{b}}{Rm} + \frac{\partial \vec{v}}{\partial z} \quad 1a-26$$

$$\nabla \cdot \vec{b} = 0 \quad 1a-27$$

$$\nabla \cdot \vec{v} = 0 \quad 1a-28$$

The boundary conditions on the pressure at the free surface becomes

$$p(x, \zeta, t) = \delta(x) \delta(t) \quad 1a-29$$

All other boundary conditions are unchanged.

Since the boundary conditions are in terms of  $\vec{v}, \zeta, p$  and  $\vec{b}$  instead of  $j$  and  $\omega$ , we require at least two functions to solve the problem, one of which must be rotational.

We introduce a harmonic function  $\phi$ , and the magnetic potential  $\vec{A}$ ; with an appropriate choice of  $\phi$ , all quantities can be expressed simply in terms of  $A$  and  $\phi$ .

$\vec{A}$  is defined by

$$\vec{A} = \Gamma_y A_y = \Gamma_y A(x, z, t) \quad 1a-30$$

and the perturbation magnetic field is given by

$$b_x = \frac{\partial A}{\partial z} ; b_z = -\frac{\partial A}{\partial x} \quad 1a-31$$

In terms of A equation 1a-25 is

$$\frac{\partial v_z}{\partial t} = -\frac{\partial p}{\partial z} - 1 \quad 1a-32$$

$$\frac{\partial v_x}{\partial t} = -\frac{\partial p}{\partial x} + \alpha^2 \nabla^2 A$$

Hence, by equations 1a-32, 1a-27 and 1a-28

$$\nabla^2 (p - \alpha^2 \frac{\partial A}{\partial x}) = 0$$

Hence we define  $\phi$  to be

$$p = \alpha^2 \frac{\partial A}{\partial x} + \phi - z \quad 1a-33$$

The velocities are found to be, by equation 1a-32

$$\frac{\partial v_z}{\partial t} = -\alpha^2 \frac{\partial^2 A}{\partial z \partial x} - \frac{\partial \phi}{\partial z} \quad 1a-34$$

$$\frac{\partial v_x}{\partial t} = \alpha^2 \frac{\partial^2 A}{\partial z^2} - \frac{\partial \phi}{\partial x}$$

If  $\alpha = 0$ ,  $\frac{\partial \phi}{\partial t}$  would be the classical velocity potential.

The vorticity is given by

$$\frac{\partial \omega}{\partial t} - \alpha^2 \nabla^2 \frac{\partial A}{\partial z} = 0 \quad 1a-35$$

This is exactly equation 1a-17. Hence, in terms of  $\phi$ ,  $A$ , all the Alfvén wave structure of the problem should be in  $A$ . Introducing  $A$ ,  $\phi$  into the induction equation 1a-26 we find

$$\frac{\partial^2 A}{\partial t^2} - \alpha^2 \frac{\partial^2 A}{\partial z^2} = \frac{\partial}{\partial t} \frac{\nabla^2 A}{Rm} - \frac{\partial \phi}{\partial x} \quad 1a-36$$

This equation, with the fact that  $\phi$  is harmonic

$$\nabla^2 \phi \equiv \left( \frac{\partial^2}{\partial x^2} + \frac{\partial^2}{\partial z^2} \right) \phi = 0$$

are the two equations to be solved. The boundary conditions at the surface are

$$\alpha^2 \frac{\partial A}{\partial x}(x, 0, t) + \phi(x, 0, t) - h(x, t) = f(x) g(t) \quad 1a-37$$

$$\frac{\partial^2 h(x, t)}{\partial t^2} = -\alpha^2 \frac{\partial^2 A}{\partial z \partial x}(x, 0, t) - \frac{\partial \phi}{\partial z}(x, 0, t) \quad 1a-38$$

Or, upon eliminating  $\zeta$  from equations 1a-37 and 1a-38 we find

$$\left( \frac{\partial^2}{\partial t^2} + \frac{\partial}{\partial z} \right) \phi + \alpha^2 \frac{\partial}{\partial x} \left( \frac{\partial^2}{\partial t^2} + \frac{\partial}{\partial z} \right) A = f''(t) f(x) \quad 1a-39$$

The magnetic boundary conditions at the surface state that  $A$  and  $\frac{\partial A}{\partial z}$  are continuous at  $z = 0$ . Above the surface ( $z > 0$ )  $A$  is harmonic.  $A, \phi \rightarrow 0$  as  $|z| \rightarrow \infty$ .

To find an integral representation of the solution, we form the Fourier transform with respect to  $x$  and the Laplace transform with respect to time, i. e.

$$\phi(x, z, t) = \frac{1}{4\pi^2 i} \int_{-i\infty}^{i\infty} e^{st} ds \int_{-\infty}^{\infty} e^{ikx} \tilde{\phi}(s, k) dk \quad 1a-40$$

$$\tilde{\phi}(s, k) = \int_{-\infty}^{\infty} e^{-ikx} \int_0^{\infty} e^{-st} \phi(x, z, t) dt dx \quad 1a-41$$

where  $k$  is real.

$$\phi = \tilde{\phi}(s, k) e^{|k|z} \quad 1a-42$$

and, for  $z < 0$ ,  $\tilde{A}$  satisfies

$$s^2 \tilde{A} - \alpha^2 \frac{\partial^2 \tilde{A}}{\partial z^2} = \frac{s}{Rm} \left( -k^2 \tilde{A} + \frac{\partial^2 \tilde{A}}{\partial z^2} \right) - ik \tilde{\phi}(s, k) e^{|k|z} \quad 1a-43$$

The appropriate solution for  $A$  is

$$\tilde{A} = a(s, k) \exp z \left| \sqrt{\frac{s^2 + sk^2/Rm}{\alpha^2 + s/Rm}} \right| + \frac{ik \tilde{\phi}(s, k) e^{|k|z}}{k^2 \alpha^2 - s^2} \quad 1a-44$$

For  $z > 0$ ,  $\tilde{A}$  is

$$\tilde{A} = B(s, k) e^{-|k|z} \quad 1a-45$$

The representations of  $\phi$ ,  $A$  given by equations 1a-42, 1a-44 and 1a-45 satisfy the boundary conditions at  $|z| = \infty$ .

Transformed equation 1a-39 becomes

$$\left(s^2 + \frac{\partial}{\partial z}\right) \tilde{\phi} + ik\alpha^2 \left(s^2 + \frac{\partial}{\partial z}\right) \tilde{A} = s^2 \quad \text{1a-46}$$

Hence to find  $a$ ,  $B$ ,  $\tilde{\phi}$  we use the fact that  $A$  and  $\frac{\partial A}{\partial z}$  are continuous at  $z = 0$ , and equation 1a-46. The resulting equations for  $a$ ,  $\tilde{\phi}$ ,  $B$  are:

$$a \left| \sqrt{\frac{s^2 + sk^2/Rm}{\alpha^2 + s/Rm}} \right| + \frac{ik|k|\tilde{\phi}}{k^2\alpha^2 - s^2} = -|k|B \quad \left(\frac{\partial A}{\partial z} \text{ cont.}\right)$$

$$a + \frac{ik\tilde{\phi}}{k^2\alpha^2 - s^2} = B \quad (A \text{ cont.})$$

$$\left(1 - \frac{k^2\alpha^2}{k^2\alpha^2 - s^2}\right) (s^2 + |k|)\tilde{\phi} + ik\alpha^2 a \left(s^2 + \left| \sqrt{\frac{s^2 + sk^2/Rm}{\alpha^2 + s/Rm}} \right| \right) = s^2 \quad \text{(1a-46)}$$

We find the function analogous to  $H(s, k)$  in Section II to be

$$H(s, k) = s^2(s^2 + |k|) \left( |k| + \left| \sqrt{\frac{s^2 + sk^2/Rm}{\alpha^2 + s/Rm}} \right| \right) - 2k^2|k|\alpha^2 \left( s^2 + \left| \sqrt{\frac{s^2 + sk^2/Rm}{\alpha^2 + s/Rm}} \right| \right) \quad \text{1a-47}$$

Solving for  $a$ ,  $\tilde{\phi}$ ,  $B$ , we find

$$a = \frac{2ik|k|s^2}{H(s, k)} \quad \text{1a-48}$$

$$\Phi = -\frac{s^2}{H(s,k)} (k^2 \alpha^2 - s^2) \left( |k| + \sqrt{\frac{s^2 + s k^2 / Rm}{\alpha^2 + s / Rm}} \right) \quad 1a-49$$

$$B = \frac{i k s^2}{H(s,k)} \left( |k| - \sqrt{\frac{s^2 + s k^2 / Rm}{\alpha^2 + s / Rm}} \right) \quad 1a-50$$

Hence from equation 1a-44 we find

$$\tilde{A} = \frac{s^2 i k}{H} \left\{ 2 |k| e^{z \sqrt{\frac{s^2 + s k^2 / Rm}{\alpha^2 + s / Rm}}} - \left( |k| + \sqrt{\frac{s^2 + s k^2 / Rm}{\alpha^2 + s / Rm}} \right) e^{|k| z} \right\} \quad 1a-51$$

and finally, from equation 1a-38

$$\tilde{f} = \frac{|k|}{H} \left\{ 2 \alpha^2 k^2 \sqrt{\frac{s^2 + s k^2 / Rm}{\alpha^2 + s / Rm}} - s^2 \left( |k| + \sqrt{\frac{s^2 + s k^2 / Rm}{\alpha^2 + s / Rm}} \right) \right\} \quad 1a-52$$

The equations 1a-47 through 1a-52 are an integral representation of the solution in the sense of equation 1a-40.



### C. The Limiting Case of Infinite Conductivity

Here we consider the limiting case of  $Rm \rightarrow \infty$ , as an aid to constructing the general solution with  $Rm$  finite. In this case, equations 1a-25 through 1a-28 become

$$\frac{\partial \vec{v}}{\partial t} = -\nabla p + \alpha^2 \text{curl } \vec{b} \times \vec{1}_z - \vec{1}_z \quad 1a-53$$

$$\frac{\partial \vec{b}}{\partial t} = \frac{\partial \vec{v}}{\partial z} \quad 1a-54$$

$$\text{div } \vec{b} = \text{div } \vec{v} = 0 \quad 1a-55$$

the only change being the omission of the diffusion term  $\frac{\nabla^2 \vec{b}}{Rm}$  in the induction equation. The boundary conditions at the free surface and at  $z = +\infty$  are unchanged; at  $z = -\infty$ , we can only specify that the solution is bounded, due to the possibility of undamped Alfvén wave propagation.

The radical

$$\left| \sqrt{\frac{s^2 + s k^2 / Rm}{\alpha^2 + s / Rm}} \right|$$

evidently becomes

$$|s/\alpha| = +\frac{s}{\alpha}$$

where the plus sign must be chosen to have  $\text{Re} \left| \frac{s}{\alpha} \right| > 0$  on the contour of integration. The functions  $A$ ,  $\phi$  then become

$$\tilde{A} = \frac{s^2 i k}{H} \left\{ 2|k| e^{z s/\alpha} - (|k| + \frac{s}{\alpha}) e^{z|k|} \right\} \quad 1a-56$$

and

$$\tilde{\phi} = -\frac{s^2}{H} (k^2 \alpha^2 - s^2) (|k| + \frac{s}{\alpha}) e^{z|k|} \quad 1a-57$$

where H now is

$$H(s, k) = s^2 (s^2 + |k|) (|k| + \frac{s}{\alpha}) - 2k^2 |k| \alpha^2 (s^2 + \frac{s}{\alpha}) \quad 1a-58$$

Finally, we find  $\tilde{\zeta}$  to be

$$\tilde{\zeta} = \frac{1}{H} \{ 2 \alpha^2 k^2 |k| \frac{s}{\alpha} - s^2 |k| (|k| + \frac{s}{\alpha}) \} \quad 1a-59$$

We note that now  $H(s, k)$  is a polynomial (Eq. 1a-58). Considerable simplification results from the fact that it may be factored:

$$H(s, k) = s (s - |k|\alpha) ( \frac{s^3}{\alpha} + 2|k|s^2 + s(\frac{|k|}{\alpha} + 2k^2\alpha) + 2k^2 ) \quad 1a-60$$

Examination of equations 1a-56, 1a-57 and 1a-59 shows that  $\tilde{\zeta}$ ,  $\tilde{\phi}$  and  $\tilde{A}$  have no poles at  $s = 0$ ,  $s = |k|\alpha$ . Hence we introduce a new function

$$F(s, k) = \frac{s^3}{\alpha} + 2|k|s^2 + s(\frac{|k|}{\alpha} + 2k^2\alpha) + 2k^2 \quad 1a-61$$

Then  $\tilde{\zeta}$  becomes

$$\tilde{\zeta} = \frac{k^2 (2 + \frac{s}{\alpha|k|})}{F(s, k)} ; \quad 1a-62$$

and

$$\tilde{\phi} = -\frac{s (s + \alpha|k|) (|k| + \frac{s}{\alpha}) e^{z|k|}}{F(s, k)} \quad 1a-63$$

and

$$\tilde{A} = \frac{ik s}{(s - |k|\alpha)F} 2|k| e^{z s \alpha} - (|k| + \frac{s}{\alpha}) e^{z|k|} \quad 1a-64$$

Now  $F$  has one real negative root, and two complex conjugate roots.

Let  $a(|k|)$ ,  $b(|k|)$ ,  $c(|k|)$  be real, positive functions of  $|k|$ . Then

$$F = \frac{1}{\alpha} (s + c) (s + a - ib) (s + a + ib) \quad 1a-65$$

For  $|k| \rightarrow 0$

$$F \sim \frac{1}{\alpha} (s + 2|k|\alpha) (s - i\sqrt{|k|(1+2\alpha^2|k|)}) (s + i\sqrt{|k|(1+2\alpha^2|k|)}) \quad 1a-66$$

and for  $|k| \rightarrow \infty$ ,

$$F \sim 2 \left( \frac{s}{\alpha} + 1 \right) (s + |k|\alpha(1-i)) (s + |k|\alpha(1+i)) \quad 1a-67$$

This completes the description of  $\tilde{A}$ ,  $\tilde{\phi}$ ,  $\tilde{\zeta}$ . We next turn to the problem of constructing approximations to  $\phi$ ,  $A$  and  $\zeta$  for large  $t$ ,  $x$ ,  $-z$ . Now the most interesting physical quantities are the surface shape  $\zeta$ , and the magnetic field vector potential  $A$ . We begin with  $A$

$$A = \frac{1}{4\pi^2 i} \int_{-\infty}^{\infty} e^{ikx} \int_{-i\infty}^{i\infty} e^{st} \tilde{A} ds dk \quad 1a-68$$

Remembering that  $\text{Res}(\tilde{A}(s = |k|\alpha)) = 0$ , we may use equation 1a-64 and write

$$A \sim \frac{1}{4\pi^2 i} \int_{-\infty}^{\infty} ike^{ikx} \int_{-i\infty}^{i\infty} \frac{se^{st+z s/\alpha}}{(s-|k|\alpha)F} ds dk \quad 1a-69$$

as  $z \rightarrow -\infty$ . Now the contour integration in equation 1a-69 is performed as follows:

For  $t + z/\alpha < 0$ , we form the contour consisting of a large semi-circle to the right of  $s = 0$ . Letting the radius of the semi-circle become large, the integral on the semi-circle goes to zero. But this contour encloses no poles. Hence

$$A \sim 0 \text{ for } t + z/\alpha < 0 \text{ and } z \rightarrow -\infty \quad 1a-70$$

For  $t + z/\alpha > 0$ , we form the contour consisting of a large semi-circle to the left of  $s = 0$ . This contour encloses three poles, at  $s = -c$ , and  $s = -a \pm ib$ . Further, as the radius of the semi-circle gets large, the integral on the semi-circle goes to zero. Hence

$$A \sim \frac{1}{2\pi} \int_{-\infty}^{\infty} i k e^{i k x} dk \left\{ \text{Res } \tilde{A}(s = -c) + \text{Res } \tilde{A}(s = -a + ib) + \text{Res } \tilde{A}(s = -a - ib) \right\} \quad 1a-71$$

for  $z \rightarrow -\infty$ , and  $t + z/\alpha > 0$ . The first term in the brackets of equation 1a-71 may be estimated as follows:

The dominant contribution to an integral of this form

$$\lim_{t \rightarrow \infty} \int_{-\infty}^{\infty} e^{i k x} e^{-c(k)t} dk$$

occurs at  $c(k) \sim 0$ . Using equation 1a-66 we find that

$$\frac{1}{2\pi} \int_{-\infty}^{\infty} i k e^{i k x} dk \left\{ \text{Res } \tilde{A}(s = -c) \right\} = \frac{1}{3\pi} \int_0^{\infty} \frac{\sin k x dk}{k(1 + 6\alpha^2 k)} e^{-2k\alpha(t + z/\alpha)} \quad 1a-72$$

Writing this function as a derivative with respect to  $x$ , and then integrating by parts, we find

$$\frac{1}{2\pi} \int_{-\infty}^{\infty} i k e^{i k x} dk \{ \text{Res } \tilde{A}(s=-c) \} = \frac{1}{3\pi} \int_0^{\infty} \frac{\sin k x dk e^{-2k\alpha(t+z/\alpha)}}{k(1+6\alpha^2 k)} \quad 1a-73$$

as  $t, x, -z \rightarrow \infty$ , and  $t + z/\alpha > 0$ .

Hence we have

$$\frac{1}{3\pi} \int_0^{\infty} \frac{\sin k x dk e^{-2k\alpha(t+z/\alpha)}}{k(1+2\alpha^2 k)} \sim \frac{2\alpha}{3\pi} \frac{x(t+z/\alpha)}{[x^2 + 4\alpha^2(t+z/\alpha)^2]^{3/2}} \quad 1a-74$$

as  $x, -z, t \rightarrow \infty$  and  $t + z/\alpha > 0$ .

Next, we turn to the residues at  $s = -a \pm ib$ . We assume the dominant contribution to be when  $k \rightarrow 0$ . Then to lowest order,  $s = \pm ib = \pm i\sqrt{|k|}$ . We find that

$$\frac{1}{2\pi} \int_{-\infty}^{\infty} i k e^{i k x} dk \{ \text{Res } \tilde{A}(s = -a \pm ib) \} = \frac{1}{\pi} \int_0^{\infty} \sin k x \cos \sqrt{k}(t+z/\alpha) dk \quad 1a-75$$

under this assumption.

For  $t, x \rightarrow \infty$  and  $t + z/\alpha > 0$ , the method of stationary phase may be used upon equation 1a-75. We find

$$\frac{1}{2\pi} \int_{-\infty}^{\infty} i k e^{i k x} dk \{ \sum \text{Res } \tilde{A}(s = -a \pm ib) \} \sim \frac{t+z/\alpha}{2\sqrt{2\pi x}} \sin\left[\frac{(t+z/\alpha)^2}{4x} - \frac{\pi}{4}\right] \quad 1a-76$$

as  $t, x \rightarrow \infty$ ,  $t + z/\alpha > 0$ , and  $\frac{(t + z/\alpha)^2}{x} \rightarrow \infty$ . To equation 1a-76 we amend the requirement that point of stationary phase,  $k_0$ , is small:

$$k_0 = \frac{(t + z/\alpha)^2}{4x} \rightarrow 0$$

Next, we turn to the surface shape,  $\zeta(x, t)$ . Assuming the dominant contribution to  $\zeta(x, t)$  occurs when  $k$  is small, as  $t, x \rightarrow \infty$  gives

$$\begin{aligned} f(x, t) &\sim \frac{1}{4\pi^2 i} \int_{-\infty}^{\infty} |k| e^{ikx} dk \int_{-\infty}^{\infty} \frac{e^{st} ds}{(s - i\sqrt{|k|})(s + i\sqrt{|k|})} \\ &= \frac{1}{\pi} \int_0^{\infty} \sqrt{k} \cos kx \cos(\sqrt{k}t - \frac{\pi}{2}) dk \\ &\sim \frac{1}{4\sqrt{2}\pi} \frac{t^2}{x^{5/2}} \sin\left(\frac{t^2}{4x} - \frac{\pi}{4}\right) \end{aligned}$$

1a-78

as  $t/x \rightarrow 0$ ,  $t, x \rightarrow \infty$ , and  $t^2/x \rightarrow \infty$ . We compare this result with the equivalent formula for equation 1a-76:

$$A \sim \frac{t + z/\alpha}{2\sqrt{2}\pi x} \sin\left(\frac{(t + z/\alpha)^2}{4x} - \frac{\pi}{4}\right)$$

We conclude that the pole at  $s = -c$  represents an Alfvén wave which dies off algebraically as  $x, t, -z$  increase. This term is largest near  $x = 0$ , for  $t$  large.

The poles at  $s = -a \pm ib$  are more interesting. They represent a surface wave analogous to an ordinary gravity wave, which, as it propagates across the surface, emits Alfvén waves of the same frequency. This emission process causes the surface wave to be damped, which in turns damps the Alfvén wave. Hence the interaction

represented by a surface wave emitting an Alfvén wave causes damping. Evidently the complexity of  $F(s, k)$  is due to the complicated nature of this interaction.

For  $R_m$  finite, we must add diffusion to the above picture. This changes the effect of radiation damping on the surface wave. Also, we expect the sharp wave front at  $t + z/\alpha = 0$  to be smeared out, due to diffusion.

D. The Functions  $H(s, k)$  and  $\sqrt{\frac{s^2 + s k^2 / Rm}{\alpha^2 + \frac{s}{Rm}}}$

We turn now to the case of  $Rm$  finite. Then instead of a dispersion relation  $F(s, k)$  (Eq. 1a-61) which is a polynomial in  $s$  and  $k$ , we have a more complicated function,  $H(s, k)$  given by equation 1a-47. Since

$$H(s, k) = H(s, -k) = H(s, |k|)$$

we may as well consider  $k \geq 0$ . The branch cuts which occur due to the radical

$$\sqrt{\frac{s^2 + s k^2 / Rm}{\alpha^2 + s / Rm}}$$

must be chosen such that, on the contour of integration,  $s = \eta + i\omega$ ,  $\eta = \text{const} > 0$ ; we have

$$\text{Re} \sqrt{\frac{s^2 + s k^2 / Rm}{\alpha^2 + s / Rm}} > 0 \quad 1a-79$$

Equation 1a-79 determines uniquely the branch cuts to be as follows: from  $s = 0$ ,  $s = -k^2 / Rm$  and  $s = \alpha^2 Rm$ , the branch cuts run along  $\text{Re} s < 0$ ,  $\text{Im} s = 0$  to  $s = -\infty$ . With this choice of branch cuts, and  $k$  positive, we may drop the bars on  $k$  and the radical and write equation 1a-47 as:

$$H(s, k) = s^2 (s^2 + k) \left( k + \sqrt{\frac{s^2 + s k^2 / Rm}{\alpha^2 + s / Rm}} \right) - 2 k^3 \alpha^2 \left( s^2 + \sqrt{\frac{s^2 + s k^2 / Rm}{\alpha^2 + \frac{s}{Rm}}} \right) \quad 1a-80$$



Following the structure of the case of  $R_m \rightarrow \infty$ , we should first determine the number of zeros of  $H(s, k)$ . Since  $H(s, k)$  is not a polynomial, this is not a simple job. There are no simple conformal mappings  $s = f(\theta)$  which map the branch cuts into the unit circle and keep  $s = f(\theta)$  an analytic function of  $\theta$ . Setting  $H(s, k) = 0$ , and squaring out the radical gives a tenth order polynomial; hence  $H$  must have at most ten zeros. Examination of  $H(s, k) = 0$  for  $\text{Im}s = 0$  reveals that there are three real zeros of  $H$ . In addition,  $H$  has two zeros which are complex conjugate. Hence, in general,  $H$  has at least five zeros. From the case  $R_m \rightarrow \infty$ , we expect that  $H$  has only five zeros, but this is not proven.

Two of the real zeros of  $H(s, k)$  are trivial in that  $\bar{A}$ ,  $\bar{\phi}$  and  $\bar{\zeta}$  do not have poles at these points. They are

$$s = 0 \text{ and } s = |k| \alpha \quad 1a-81$$

For construction of approximate solutions, it is necessary to know the zeros of  $H(s, k)$  for large and small  $k$ . These are, in addition to those of equation 1a-81:

For  $k \rightarrow 0$ :

$$\left. \begin{aligned} s &= -2|k|\alpha + O(k^2) \\ s &= \pm i \sqrt{|k|(1 + 2\alpha^2|k|)} + O(k^{5/2}) \end{aligned} \right\} \quad 1a-82$$

For  $k \rightarrow \infty$ :

$$\left. \begin{aligned} s &= -|k|\alpha + O(1) \\ s &= -\frac{\alpha^2 R_m}{4} \pm i \sqrt{|k|} + O\left(\frac{1}{\sqrt{k}}\right) \end{aligned} \right\} \quad 1a-83$$

This completes the discussion of  $H(s, k)$ .

We next turn to study the radical,  $\sqrt{\frac{s^2 + s k^2 / Rm}{\alpha^2 + s / Rm}}$ . The conductivity,  $Rm$ , appears only in this radical. Consider the limiting cases  $k \rightarrow 0$ ,  $k \rightarrow \infty$  with  $O(s)$  between  $O(|k|)$  and  $O(k)$ :

$$\lim_{k \rightarrow \infty} \sqrt{\frac{s^2 + s k^2 / Rm}{\alpha^2 + s / Rm}} = k ;$$

1a-84

$$O(\sqrt{k}) < s < O(k)$$

$\alpha$ ,  $Rm$  fixed

and

$$\lim_{k \rightarrow 0} \sqrt{\frac{s^2 + s k^2 / Rm}{\alpha^2 + s / Rm}} = \frac{s}{\alpha}$$

$$k \rightarrow 0$$

1a-85

$$O(k) < s < O(\sqrt{k})$$

We may formally produce the same results by considering

$$\lim_{Rm \rightarrow 0} \sqrt{\frac{s^2 + s k^2 / Rm}{\alpha^2 + s / Rm}} = k$$

1a-86

$\alpha$ ,  $s$ ,  $k$  fixed

and

$$\lim_{Rm \rightarrow \infty} \sqrt{\frac{s^2 + s k^2 / Rm}{\alpha^2 + s / Rm}} = \frac{s}{\alpha}$$

1a-87

$\alpha$ ,  $s$ ,  $k$  fixed

Thus, the zeros of  $H(s, k)$  which are such that  $O(s)$  is between

$O(\sqrt{k})$  and  $O(k)$  as  $k \rightarrow \infty$  or  $k \rightarrow 0$  must agree to first order, when  $k$  is small or large, with the approximate zeros formed by  $\lim_{R_m \rightarrow 0} H$  and  $\lim_{R_m \rightarrow \infty} H$ .

Reviewing the case of  $R_m \rightarrow \infty$ , we see that the complex zeros which represent a traveling surface wave emitting an Alfvén wave are of this class. Hence, for the surface-wave emission coupling we may expect, from equations 1a-84 through 1a-87, that certain portions of the surface wave are regions of high effective conductivity, and other portions are regions of low effective conductivity.

### E. The Alfvén Wave Structure

We consider, as in the case of  $Rm \rightarrow \infty$ , only the part of the magnetic vector potential  $A$  which contains the Alfvén wave structure. In doing this we recall that  $\tilde{A}$  has no pole at  $s = |k| \alpha$ . From equations 1a-44, 1a-48 and 1a-51 we have:

$$A \approx \frac{1}{4\pi^2 i} \int_{-\infty}^{\infty} ik e^{ikx} dk \int_{-i\infty}^{i\infty} \frac{s^2/k^2}{H(s,k)} e^{st} e^{z \sqrt{\frac{s^2 + sk^2/Rm}{\alpha^2 + s/Rm}}} ds \quad 1a-88$$

In equation 1a-88 we have neglected the harmonic part of  $A$ , as it plays no role in the Alfvén wave structure.

We next wish to show that there is a critical wave number,  $\tilde{k}$ , such that for  $k > \tilde{k}$ , diffusion is the dominant feature of equation 1a-88, and for  $k < \tilde{k}$ , wave propagation is a feature of the equation. To find  $\tilde{k}$ , we note that for  $k^2/Rm < \alpha^2 Rm$ , there is a region in the complex  $s$  plane such that  $\text{Re} \sqrt{\frac{s^2 + sk^2/Rm}{\alpha^2 + s/Rm}} < 0$ . This region lies to the left of the line  $s = -k^2/Rm$ . If  $A$  has a pole in this region, then for small  $k$ , its structure is like that of a wave propagating down. Clearly, all the poles of  $A$  for  $Rm \rightarrow \infty$  fall in this class.

On the other hand, for  $k^2/Rm > \alpha^2 Rm$ ,  $\text{Re} \sqrt{\frac{s^2 + sk^2/Rm}{\alpha^2 + s/Rm}} > 0$  in the left half plane. Hence any pole of  $A$  represents a disturbance with exponential decay or algebraic decay in  $z$ . Under these circumstances there is no wave propagation. Hence we set

$$\tilde{k} = \alpha Rm \quad 1a-89$$

For this value of  $\tilde{k}$ , the term  $\frac{\partial^2 A}{\partial t^2}$  is exactly 90 degrees out of phase with the term  $\alpha \frac{\partial^2 A}{\partial z^2}$  in equation 1a-36, the governing equation of  $A$ .

Now we turn to asymptotic approximations for A. First we consider  $t, z \rightarrow \infty$ . From the above discussion, we need only consider three cases:  $k \rightarrow 0$ ,  $k = \tilde{k}$  and  $k \rightarrow \infty$ . In these cases we shall evaluate:

$$F(k) = \frac{1}{2\pi i} \int_{-i\infty}^{i\infty} \frac{s^2 e^{st}}{H} e^{z \sqrt{\frac{s^2 + sk^2/Rm}{\alpha^2 + s/Rm}}} ds \quad 1a-90$$

by using the method of steepest descent. With this done, we shall quantitatively examine

$$A = \frac{1}{2\pi} \int_{-\infty}^{\infty} i k e^{ikx} F(k) dk.$$

For  $k \rightarrow 0$ , we write

$$f(s) = st + z \sqrt{\frac{s^2 + sk^2/Rm}{\alpha^2 + s/Rm}}$$

as

$$f(s) \doteq st + \frac{zs}{\sqrt{\alpha^2 + s/Rm}}$$

The dominant saddle point is when  $|s| \ll 1$ :

$$f'(s_0) = 0 \doteq t + \frac{z}{\alpha} \left( 1 - \frac{1}{2} \frac{s_0}{\alpha^2 Rm} \right)$$

Hence

$$s_0 = \frac{2\alpha^2 Rm}{z/\alpha} \left( t + \frac{z}{\alpha} \right)$$

Then  $|s_0| \ll 1$  implies

$$t \doteq -z/\alpha$$

Hence

$$s_0 = -\frac{2\alpha^2 Rm}{t} \left( t + \frac{z}{\alpha} \right)$$

Then we find

$$f''(s_0) = \frac{t}{2\alpha^2 Rm} \quad 1a-92$$

Hence the path of steepest descent is parallel to the  $\text{Im}s$  axis, and goes through  $s = s_0$ .

Hence we find

$$\lim_{k \rightarrow 0} F(k) \sim \frac{1}{4\sqrt{\pi}} \sqrt{\frac{2\alpha^2 Rm}{t}} \frac{s_0^2}{H(s_0, k)} e^{-\frac{(t+z/\alpha)^2 2\alpha^2 Rm}{t}} \quad 1a-93$$

Equation 1a-93 describes the propagation of a plane Alfvén wave propagating with a speed  $\alpha$ , and diffusing isotropically about the wave front.

For  $k = \tilde{k}$ ,  $f(s)$  becomes

$$f(s) = st + z\sqrt{s Rm} \quad 1a-94$$

The saddle point is

$$s_0 = \left(\frac{z}{2t}\right)^2 Rm \quad 1a-95$$

We find

$$f''(s_0) = \frac{2t^3}{z^2 Rm}$$

hence the path of steepest descent is parallel to the  $\text{Im}s$  axis, and runs through  $s = s_0$ . Hence

$$F(\tilde{k}) \sim \frac{1}{2} \sqrt{\frac{Rm}{2\pi t}} \left(\frac{z}{t}\right)^2 e^{-\frac{z^2}{2t} Rm} \frac{s_0^2}{H(s_0, k)} \quad 1a-96$$

as  $-z, t \rightarrow \infty$ . Equation 1a-96 describes the "propagation" of a diffusive hump, which has a maximum at  $z = \sqrt{\frac{t}{Rm}}$ , the velocity of the maximum is  $\frac{dz}{dt} = \frac{1}{2\sqrt{Rm t}}$ . Hence there is no definite speed of propagation, and no Alfvén wave.

For  $k \rightarrow \infty$ ,  $t(s)$  becomes

$$f(s) = st + zk \sqrt{\frac{s}{\alpha^2 Rm + s}} \quad 1a-97$$

For  $z/t \sim O(1)$  as  $-z, t \rightarrow \infty$ , and  $k \rightarrow \infty$ , we find the saddle point to be

$$s_0 = \sqrt{\frac{(-z)k\alpha^2 Rm}{t}} \quad 1a-98$$

and

$$f''(s_0) = \frac{2t}{\sqrt{\frac{(-z)k\alpha^2 Rm}{2t}}} \quad 1a-99$$

Hence, the path of steepest descent is again parallel to the  $\text{Im}s$  axis passing through  $s = s_0$ . We find

$$\lim_{k \rightarrow \infty} F(k) \sim \frac{1}{2\sqrt{2\pi t}} \left( \frac{|z|k}{t\alpha^2 Rm} \right)^{1/4} e^{kz} e^{\sqrt{\frac{|z|}{2} t k \alpha^2 Rm}} \frac{S_0^2}{H(S_0, k)} \quad 1a-100$$

Equation 1a-100 also describes a diffusive hump whose maximum is located at  $z = \left( \frac{t}{8} \frac{\alpha^2 Rm}{k} \right)^{2/3}$  for large  $k$ , and this maximum travels with a velocity

$$\frac{dz}{dt} = \frac{2}{3} \left( \frac{\alpha^2 Rm}{8k} \right)^{2/3} \left( \frac{1}{t} \right)^{1/3}$$

The equations 1a-93, 1a-96 and 1a-100 serve to clarify the nature of  $\bar{k}$ . Turning to the integral

$$\frac{1}{2\pi} \int_{-\infty}^{\infty} e^{ikx} F(k) ik dk = \frac{1}{\pi} \int_0^{\infty} k \sin kx F(k) dk$$

we see that if for some value of  $x$ ,  $t$ ,  $z$  this integral has its main contribution for  $0 < k < \tilde{k}$ , then the result will be an Alfvén wave propagating down with some  $x$  variation. If the main contribution to the integral comes for  $\tilde{k} < k < \infty$ , there will be no Alfvén wave propagation.

Clearly, the limit  $Rm \rightarrow \infty$  can only be valid for wave numbers less than  $\tilde{k} = \alpha Rm$ . For mercury at 10,000 gauss,  $\tilde{k} = \frac{6}{\text{meters}}$ .

Next, we assume that the dominant contribution to  $A$  comes when  $k \rightarrow 0$ . In this case  $A$  has poles at  $s = -2|k|\alpha$ ,  $s = i\sqrt{|k|(1+2\alpha^2|k|)}$ , and  $s = -i\sqrt{|k|(1+2\alpha^2|k|)}$  (Eq. 1a-82). For the three poles, equations 1a-84 through 1a-87 apply, hence we may use the results of the previous section on  $Rm \rightarrow \infty$  (Eqs. 1a-74 and 1a-76).

$$A \sim \frac{2\alpha}{3\pi} \frac{x(t+z/\alpha)}{[x^2 + 4\alpha^2(t+z/\alpha)^2]^{3/2}} + \frac{t+z/\alpha}{2\sqrt{2\pi}x} \operatorname{erfc}\left(\frac{(t+z/\alpha)^2}{4x}\right) - \frac{\pi}{4} \quad 1a-101$$

as  $x, t \rightarrow \infty$ ;  $t + z/\alpha > 0$ ; and  $\frac{t+z/\alpha}{x} \rightarrow 0$ .

The approximations (Eq. 1a-101) were derived under the assumption that the dominant contribution to  $A$  occurs for  $k \rightarrow 0$ . This assumption fixed the region of validity of the resulting approximations in  $(x, z, t)$  space.

We now turn to the case where  $A$  has its dominant contribution for  $k \rightarrow \infty$ . Reviewing equation 1a-83, we see that only the poles at  $s = -\frac{\alpha^2 Rm}{4} \pm i\sqrt{|k|}$  can meet this requirement.



In this case

$$A \sim \frac{1}{\pi} \int_0^{\infty} \frac{k^3}{\sqrt{k}} \sin kx \, dk \, e^{-\frac{\alpha^2 R m t}{4}} \cos \sqrt{k} t e^{kz}$$

This integral may be approximated, for  $z$  fixed,  $x, t \rightarrow \infty$ , and  $t^2/x \rightarrow \infty$ , by the method of stationary phase. The point of stationary phase is

$$k_0 = \frac{t^2}{4x} \rightarrow \infty$$

Hence the approximation is valid for  $\frac{t}{x} \rightarrow \infty$  as  $x, t \rightarrow \infty$ ,  $t^2/x \rightarrow \infty$ ,  $z \cdot x \rightarrow 0$ ,  $z/t \rightarrow 0$ . We find, under these conditions that

$$A \sim \frac{e^{-\frac{\alpha^2 R m t}{4}}}{\sqrt{\pi t}} \left(\frac{t}{2x}\right)^{1/2} \sin\left(\frac{t^2}{4x} - \frac{\pi}{4}\right) e^{\frac{t^2 z}{4x^2}}$$

1a-102

Before discussing the physical interpretation of these approximations to the Alfvén wave structure we find analogous results for the surface shape,  $\zeta(x, t)$ .

## F. The Surface Shape

The surface shape is given by equation 1a-52

$$h(x,t) = \frac{1}{4\pi^2 i} \int_{-\infty}^{\infty} \int_{-i\infty}^{i\infty} \frac{e^{ikx} e^{st}}{H(s,k)} \left\{ 2\alpha^2 k^2 \sqrt{\frac{s^2 + s k^2 / Rm}{\alpha^2 + s/Rm}} - s^2 (|k| + \sqrt{\frac{s^2 + s k^2 / Rm}{\alpha^2 + s/Rm}}) \right\} ds dk \quad 1a-103$$

Since we have only an  $x, t$  variation, the approximations to  $\zeta(x, t)$  are straightforward. For  $k \rightarrow 0$ ,  $\bar{\zeta}$  has poles at  $s \doteq \pm i\sqrt{|k|}$ , the denominator cancels all the other zeros of  $H$ . Let  $\zeta(x, t)$  have its dominant contribution for  $k \rightarrow 0$ . Then, from equations 1a-84, 1a-85, 1a-86, 1a-87 and the previous discussion, it follows that  $\zeta$  is given by the same formula, to lowest order in  $t/x$ , as was derived for  $Rm \rightarrow \infty$ . This is equation 1a-78

$$h(x,t) \sim \frac{1}{4\sqrt{2}\pi} \frac{t^2}{x^{5/2}} \sin\left(\frac{t^2}{4x} - \frac{\pi}{4}\right) \quad 1a-78$$

as  $t/x \rightarrow 0$ ,  $t, x \rightarrow \infty$ , and  $t^2/x \rightarrow \infty$ . We conclude that the leading edge of the surface wave, and its resulting Alfvén wave structure (Eq. 1a-101) are a region of high conductivity effects.

Assuming  $\zeta$  to have a dominant contribution when  $k \rightarrow \infty$ , we find that  $\zeta$  only has poles at  $s \doteq -\frac{\alpha^2 Rm}{4} \pm i\sqrt{|k|}$ . Then, to lowest order, we find, by contour integration and the method of stationary phase, that

$$h \sim \frac{1}{4\sqrt{2}\pi} e^{-\frac{\alpha^2 Rm t}{4}} \frac{t^2}{x^{5/2}} \sin\left(\frac{t^2}{4x} - \frac{\pi}{4}\right) \quad 1a-104$$

as  $t/x \rightarrow \infty$ ,  $x, t \rightarrow \infty$  and  $t^2/x \rightarrow \infty$ ; to first order in  $x/t$ . With this surface deflection we associate the Alfvén wave structure of equation 1a-103. We conclude that the trailing edge of the surface wave (and its Alfvén wave structure, by Eqs. 1a-84 through 1a-87) is a region of low conductivity effects. Equations 1a-78 and 1a-104 complete our study of  $\zeta(x, t)$ .

## G. Conclusions

Herein we construct a physical picture of the response to a pressure pulse. The statements for  $x/t \sim 1$  are deduced from the behavior of the solution for  $x/t \rightarrow \infty$  and  $x/t \rightarrow 0$ , as  $x, t \rightarrow \infty$ . We shall only be concerned with  $x, t$  large.

We begin by considering the surface shape. For  $x/t \rightarrow 0$ ,  $\zeta(x, t)$  oscillates, in the second approximation, as a gravity wave with slightly higher frequency. In the region where  $x/t \rightarrow \infty$ ,  $(x, t)$  behaves as if the fluid had very high conductivity. We may define a local  $\tilde{R}_m$  based upon the local wave length and phase velocity. Then for  $x/t \rightarrow \infty$ ,  $\tilde{R}_m \rightarrow \infty$ .

Now as  $x/t$  decreases, so does  $\tilde{R}_m$ , and  $\zeta$  gets a damping factor. This damping factor increases monotonically as  $x/t$  and  $\tilde{R}_m$  decrease, until for  $x/t \rightarrow 0$ , it has reached the value  $e^{-\frac{\alpha^2 \tilde{R}_m t}{4}}$ . The frequency is slightly lower than that of a gravity wave for  $x/t \rightarrow 0$ . Hence  $\tilde{R}_m \rightarrow 0$  as  $x/t \rightarrow 0$ . Therefore the trailing edge of the surface wave is one of low effective conductivity.

Associated with this gravity-like surface wave is an Alfvén wave structure. For  $x/t \rightarrow \infty$ , it consists of nearly plane Alfvén waves emitted from the surface. As these waves propagate down, they diffuse as  $\alpha^2 \tilde{R}_m$ . The wave number of these Alfvén waves is the same as the local surface wave number where they were emitted. Now, as  $x/t$  decreases, the wave number of the Alfvén wave structure decreases, until at a point where  $k = \tilde{k}$ , the diffusion across field lines is as rapid as the propagation along field lines, and hence the Alfvén structure becomes purely diffusive. If we view the surface as

having a local complex frequency, then the Alfvén structure has this same frequency. Therefore the Alfvén structure gets a damping factor as  $x/t$  decreases. For  $x/t \rightarrow 0$  this damping factor has increased to  $e^{-\frac{\alpha^2 R_m t}{4}}$ , and the Alfvén structure is purely diffusive, with a diffusive factor  $\alpha^2 R_m$ .

Hence, as the surface wave propagates over the surface, it emits an Alfvén wave with the same local frequency and wave number which propagates down as an Alfvén wave or as a diffusive wave, depending upon whether  $k \gtrsim \tilde{k}$ . This emission causes the surface to be damped, which in turn damps the Alfvén wave emitted.

Near the origin,  $x = 0$ , there is an Alfvén wave propagating down. The wave front of this Alfvén wave is smeared out due to diffusion.

Next, we study the effect of interchanging the limit process  $k \rightarrow 0$  with  $\alpha$  fixed,  $R_m \rightarrow \infty$ ; and  $k \rightarrow \infty$  with  $R_m \rightarrow 0$ ,  $\alpha^2 R_m$  fixed.

Consider only the surface shape  $\zeta(x, t)$ . We compare the results obtained by letting  $k \rightarrow 0$  with those obtained by letting  $R_m \rightarrow \infty$  with  $\alpha$  fixed. In the next appendix, Appendix II, it will be shown that such processes as  $k \rightarrow 0$  produce approximations to  $\zeta(x, t)$  which are expansions of the phase and damping of  $\zeta(x, t)$  for  $x/t$  large. The limit process  $R_m \rightarrow \infty$ ,  $\alpha$  fixed produces the same residues as the limit  $k \rightarrow 0$  to  $O(k^{5/2})$ . The disagreement occurs first in the damping, which is  $O(\frac{t^6}{x^5})$  as  $x/t \rightarrow \infty$ ;  $x, t \rightarrow \infty$ .

Similarly, the limit  $k \rightarrow \infty$  produces an expansion of the phase

and damping of  $\zeta(x, t)$  for small  $x/t$  as  $x, t \rightarrow \infty$ . The limit  $R_m \rightarrow 0$ ,  $\alpha^2 R_m$  fixed produces the same residues to  $O\left(\frac{1}{k}\right)$ . Here again, the error occurs first in the damping factor, which is  $O\left(\frac{t^3}{x}\right)$  as  $\frac{x}{t} \rightarrow 0$ ;  $x, t \rightarrow \infty$ .

APPENDIX II. The Limiting Case  $Rm \rightarrow 0$ ,  $\alpha^2 Rm \sim 1$ 

## The Response to a Pressure Pulse

In this appendix we formulate the same problem as in Appendix I for the limit  $Rm \rightarrow 0$ ,  $\alpha^2 Rm \sim 1$ . We use the simple results of this problem to clarify the mathematical nature of the approximations made in Appendix I.

From previous remarks, we know this limit to be valid for  $k \gg \tilde{k} = \alpha Rm$ , and it is a distinguished limit in the sense that it preserves the Alfvén wave structure of the surface emission.

The solution to this limiting case differs from the solution described in Appendix I only in the fact that Alfvén wave propagation is absent. In particular, the solution contains branch cuts due to the Alfvén structure. These facts, plus the simplicity of the solution, make it an ideal model for an analysis of the approximations constructed under the assumption that  $k \rightarrow 0$  or  $k \rightarrow \infty$  gives the dominant contribution to certain double integrals.

With the nondimensionalization of Appendix I, under the limit process  $\alpha^2 Rm \sim 1$ ,  $Rm \rightarrow 0$ , the equations are, for  $z < 0$ :

$$\frac{\partial \vec{v}}{\partial t} = -\nabla p + \alpha^2 Rm \vec{j} \times \vec{l}_z - \vec{l}_z \quad 2a-1$$

$$\nabla^2 \vec{b} = 0 \quad 2a-2$$

$$\nabla \cdot \vec{b} = 0 \quad 2a-3$$

$$\vec{j} = \vec{e} - v_x \vec{l}_y \quad 2a-4$$

$$\frac{\partial \vec{b}}{\partial t} = -\text{curl } \vec{e} \quad 2a-5$$

$$\nabla \cdot \vec{v} = 0 \quad 2a-6$$

and for  $z > 0$ ,

$$\nabla^2 \vec{b} = 0 \quad 2a-7$$

$$\nabla \cdot \vec{b} = 0 \quad 2a-8$$

The boundary conditions are unchanged. Since  $\vec{b}$  is continuous at  $z = 0$ , and  $b \rightarrow 0$  for  $|z| \rightarrow \infty$ , we conclude from equations 2a-2, 2a-3 and 2a-7, 2a-8 that

$$\vec{b} = 0 \quad 2a-9$$

Hence by 2a-6

$$\vec{e} = 0 \quad 2a-10$$

Hence

$$j = -v_x \quad 2a-11$$

Thus the momentum equation may be written as

$$\frac{\partial \vec{v}}{\partial t} = -\nabla p - \alpha^2 Rm v_x \vec{i}_x - \vec{i}_z \quad 2a-12$$

Hence the magnetic interaction with the fluid is expressed solely by a damping term in the horizontal momentum equation due to the fact that the conducting fluid moves across the field lines. Using equations 2a-6, 2a-12 to eliminate the velocity we find the governing partial differential equation to be

$$\frac{\partial}{\partial t} \nabla^2 p + R \frac{\partial^2 p}{\partial z^2} = 0 \quad 2a-13$$

where

$$R = \alpha^2 Rm \quad 2a-14$$



is the parameter of the limit process.

In terms of the pressure, the boundary conditions may be written as

$$p(x, \zeta, t) = \delta(x) \delta(t) \quad 1a-29$$

$$\frac{\partial \zeta}{\partial t} = -\left(\frac{\partial p}{\partial z} + 1\right)_{x, 0, t} \quad 2a-15$$

on the surface. Far below the surface

$$-\frac{\partial p}{\partial z} - 1 = 0 \quad \text{as } z \rightarrow -\infty \quad 2a-16$$

These are the boundary conditions of the problem. We recall that the  $\lambda_0$  used to nondimensionalize these equations plays no significant role in the solution. The same is true for large  $x, t$  if a real length  $a$  were given by boundary conditions near  $x = 0, t = 0$ .

The solution to the problem may be obtained by applying Fourier and Laplace transforms. We write the solution in terms of the inverse transforms. We may perform the computation using equations 2a-13, 2a-15, 2a-16 and 1a-29, or take the limit of the solution for  $Rm$  finite (Appendix I). Since the Alfvén wave structure (diffusion) has been adequately discussed for this case in Appendix I, we consider the surface shape only. We have

$$h(x, t) = \lim_{z \rightarrow 0} \left\{ -\frac{1}{4\pi^2 i} \int_{-\infty}^{\infty} \int_{-\infty}^{\infty} \frac{e^{ikx} e^{st} e^{z|k| \sqrt{\frac{s}{R+s}}}}{1 + \frac{s^2}{|k|} \sqrt{\frac{R+s}{s}}} ds dk \right\} \quad 2a-17$$

We assert that the factor  $e^{z|k| \sqrt{\frac{s}{R+s}}}$  for  $z$  small and negative plays the role of a convergence factor in equation 2a-17; we may

interchange the  $\lim_{z \uparrow 0}$  with  $\lim_{x, t \rightarrow \infty}$ . This may be seen as follows: consider  $p(x, z, t)$ . By contour integration over the  $s$  integral, and application of the method of steepest descent over the  $k$  integral, we may construct an approximation to  $p(x, z, t)$  for  $x, t \rightarrow \infty$ , and  $z$  fixed. In such a computation,  $e^{z|k|\sqrt{\frac{s}{R+s}}}$  is a slowly varying factor compared to  $e^{ikx}$  or  $e^{st}$ . Hence it plays no role in the approximation by steepest descent. Therefore, if  $\zeta(x, t)$  for  $x, t \rightarrow \infty$  is computed from the approximation to  $p(x, t)$  by equation 2a-15, it will be found that we get the same result as if the order of limits were interchanged in equation 2a-17.

Hence, for the following construction of approximations to  $\zeta(x, t)$  for  $x, t \rightarrow \infty$ , we replace equation 2a-17 by the divergent integral obtained by setting  $z = 0$  (in Eq. 2a-17).

We eliminate  $R$  in equation 2a-17 by making the transformation:

$$\begin{aligned}
 s^+ &= Rs \\
 k^+ &= k/R^2 \\
 t^+ &= t/R \\
 x^+ &= x/R^2 \\
 \zeta^+ &= R^3 \zeta
 \end{aligned}
 \tag{2a-18}$$

Substituting equation 2a-18 into 2a-17 and dropping the  $( )^+$  signs, we have

$$h(x, t) = -\frac{1}{4\pi^2 i} \int_{-\infty}^{\infty} \int_{-i\infty}^{i\infty} \frac{e^{ikx} e^{st} ds dk}{1 + \frac{s^2}{|k|} \sqrt{\frac{1+s}{s}}}
 \tag{2a-19}$$

which may be written as

$$h(x,t) = -\frac{1}{\pi} \int_0^{\infty} k \cos kx dk \left\{ \frac{1}{2\pi i} \int_{-i\infty}^{i\infty} \frac{e^{st} ds}{k + s^2 \sqrt{\frac{1+s}{s}}} \right\} \quad 2a-20$$

The branch cuts run from  $s = 1$  and  $s = 0$  to  $s = -\infty$ .

Considering equation 2a-20, we may proceed in two ways: we may write  $\zeta$  as  $\frac{\partial}{\partial x}$  of another integral, and perform the  $k$  integration. Then we would approximate the resulting  $s$  integral by the method of steepest descent. Or, we may perform the  $s$  integration first, and then approximate the  $k$  integral by the method of steepest descent. Due to the complexity of the resulting  $s$  integral when the  $k$  integral is done first, the latter approach is simplest.

We evaluate

$$\frac{1}{2\pi i} \int_{-i\infty}^{i\infty} \frac{e^{st} ds}{k + s^2 \sqrt{\frac{1+s}{s}}} \quad 2a-21$$

by contour integration. Now

$$k + s^2 \sqrt{\frac{1+s}{s}}$$

has only two zeros:

$$s = -\gamma(|k|) \pm i \omega(|k|); \operatorname{Re} \gamma, \omega > 0; \operatorname{Im} \gamma, \omega = 0$$

Hence, the residues of 2a-21 give terms like:

$$F(k) e^{-\gamma t + i \omega t} \quad 2a-23$$

The branch cut contribution is

$$\frac{1}{\pi} \int_0^1 \frac{e^{-\eta t} \eta^2 \sqrt{\frac{1-\eta}{\eta}}}{k^2 + \eta^3(1-\eta)} d\eta \quad 2a-24$$

which may be shown to be

$$\sim O\left(\frac{1}{k^2 t^{5/2}}\right) \text{ as } t \rightarrow \infty, k \neq 0 \quad 2a-25$$

by substituting  $u = \eta t$  in equation 2a-24. Hence we find that the contribution to  $\zeta(x, t)$  from the branch cut contribution is

$$\sim O\left(\frac{1}{x^2 t^{5/2}}\right) \text{ as } x, t \rightarrow \infty \quad 2a-26$$

by using the convergent representation (Eq. 2a-17) for  $\zeta(x, t)$ .

We restrict our attention now to the contribution of the residues (Eq. 2a-23): these give for  $\zeta(x, t)$ , terms like

$$\int_0^{\infty} F(k) e^{-ikx - \gamma(|k|)t + i\omega(|k|)t} dk \quad 2a-27$$

Now the integrand has a sharp maximum where

$$f'(k) = 0 \quad 2a-28$$

where  $f(k)$  is given by

$$f(k) = ikx - \gamma t + i\omega t \quad 2a-29$$

The point (or points) at which  $f'(k) = 0$  we call  $k_0(x, t)$ . Then we define the phase  $b(x, t)$  of  $\zeta(x, t)$ , as  $x, t \rightarrow \infty$ , as

$$b(x, t) = \text{Im } f(k_0) \quad 2a-30$$

and the damping of  $(x, t)$  as

$$a(x, t) = \operatorname{Re} f(k_0) \text{ as } x, t \rightarrow \infty \quad 2a-31$$

Clearly  $a$  and  $b$  exist for all  $t/x$  if and only if, for all  $k$ ,  $\zeta$  has contributions from residues due to poles located at  $s = -\gamma \pm i\omega$ . In the present case, these are the only residues which contribute to  $\zeta$ ; this is not essential.

We construct approximations to  $a(x, t)$  and  $b(x, t)$  for  $t/x$  large or small, as  $t, x \rightarrow \infty$ , by using approximations to the residues for  $k \rightarrow 0$  or  $k \rightarrow \infty$ .

For  $k \rightarrow \infty$ , the poles are located at

$$s = -\frac{1}{4} + \frac{1}{32k} \pm i\sqrt{k - \frac{3}{16}} + o\left(\frac{1}{k}\right) \quad 2a-32$$

Using equation 2a-32, and performing the contour integration, and finally using the technique of stationary phase on the resulting  $k$  integral, we find that

$$k_0 = \frac{1}{4} \frac{t^2}{x^2} + \frac{3}{16} + O\left(\frac{x}{t}\right) \quad 2a-33$$

and hence

$$h(x, t) \sim \frac{t^2}{4\sqrt{2\pi}} x^{5/2} e^{-a(x, t)} \sin\left(b(x, t) - \frac{\pi}{4}\right) \quad 2a-34$$

as  $x, t \rightarrow \infty$ ,  $t^2/x \rightarrow \infty$ , and  $t/x \rightarrow \infty$ .  $a(x, t)$  and  $b(x, t)$  are given by

$$a(x, t) \sim -\frac{1}{4}t + \frac{1}{8} \frac{x^2}{t} + O\left(\frac{x^3}{t^2}\right) \quad 2a-35$$

$$b(x, t) \sim \frac{t^2}{4x} + \frac{3x}{16} + O\left(\frac{x^2}{t}\right) \quad 2a-36$$

as  $x, t \rightarrow \infty, t/x \rightarrow \infty$ .

For  $k \rightarrow 0$ , the poles are located at

$$s = e^{\pm \frac{2\pi i}{3}} k^{2/3} \left( 1 - \frac{1}{3} e^{\pm \frac{2\pi i}{3}} k^{2/3} + \frac{1}{9} e^{\pm \frac{4\pi i}{3}} k^{4/3} \right) + O(k^{7/3}) \quad 2a-37$$

Using equation 2a-37, we find an approximation to the residues.

Applying the method of steepest descent to the resulting integrals

over  $k$ , we find that equal contributions come from the terms with

exponents  $(\exp[ ikx + e \frac{2\pi i}{3} k^{2/3} t ])$  and  $(\exp[ -ikx - e \frac{2\pi i}{3} k^{2/3} t ])$ .

Deforming the path of integration to a path of steepest descent in the

first integral exactly cancels the same deformation in the second

integral. We find:

For  $x, t \rightarrow \infty, t/x \rightarrow 0$ ,

$$\zeta(x, t) \sim -\frac{8}{27} \sqrt{2\pi t} \left(\frac{t}{x}\right)^4 e^{a(x, t)} \quad 2a-38$$

where

$$a(x, t) \sim -\frac{4}{27} \frac{t^3}{x} - \frac{16}{256} \frac{t^5}{x} + O\left(\frac{t^7}{x^3}\right) \quad 2a-39$$

$$b(x, t) \sim O\left(\frac{t^5}{x}\right) \quad 2a-40$$

and

$$k_0(x, t) \sim \pm \frac{i8}{27} \left(\frac{t}{4}\right)^3 + O\left(\frac{t^5}{x^3}\right) \quad 2a-41$$

We conclude that the leading edge of the wave is a diffusing depression which gradually changes into an oscillatory motion as  $t/x$  increases.

There is a distinguished set of coordinates  $t, x, \zeta$  which eliminate the parameter  $R = \alpha^2 R_m$  from the problem.

Approximations constructed by assuming that the dominant contribution to  $\zeta$  comes for  $k$  small or large, produce expansions of  $\zeta$ , and its damping and phase, for  $t/x$  small or large.

In Appendix I, the approximations to  $\zeta$  were constructed in the above manner, as was the Alfvén wave structure emitted from the surface. We conclude that such approximations are mathematically meaningful if  $a$  and  $b$  exist for all  $t/x$ . This depends on whether or not  $\tilde{\zeta}$  has poles at  $s$  equal to a complex conjugate function of  $k$ . Due to the complicated algebraic structure of  $\tilde{\zeta}$  (Eq. 1a-52), this is not mathematically obvious. However, physically, it is clear that  $\tilde{\zeta}$  must have such poles, for only through such poles are gravity-like oscillations of the surface produced, and this gravity effect acts on all wave numbers.

## APPENDIX III

## The Solenoid Problem

In this appendix we consider an infinitely long, vertical, cylindrical solenoid, half filled with mercury. We ask, "What is the response of the free surface, when the solenoid current is changed slightly?"

Let the inner radius of the solenoid be  $a$ , the initial current  $I_0$ , and the final current  $i_1$ . Let  $\vec{W}$ ,  $P$ ,  $\vec{B}$ ,  $\vec{J}$  and  $\vec{E}$  be the dimensional velocity, pressure, magnetic field, current density and electric field respectively. We choose cylindrical coordinates  $(R, \theta, Z)$  with the  $Z$  axis parallel to the axis of the solenoid and positive upward.  $R = a$  is the equation for the wall of the solenoid, and the free surface of the mercury is initially at  $Z = 0$ . We assume the motion to be axisymmetric.

We introduce nondimensional quantities as follows:

$$(R, \theta, Z) = a(r, \theta, z) \quad 3a-1$$

$$T = \text{time} = \sqrt{\frac{a}{g}} t \quad 3a-2$$

$$\vec{W} = \sqrt{ag} \vec{V} \quad 3a-3$$

$$\vec{E} = \sqrt{ag} B_0 \vec{e} \quad 3a-4$$

$$\vec{B} = B_0 \vec{b} \quad 3a-5$$

$$P = \rho g a p \quad 3a-6$$

$$\vec{J} = \alpha \sqrt{ga} B_0 \vec{j} \quad 3a-7$$

The parameters of the problem are:

$$Rm = \mu \sigma a \sqrt{ag} \quad 3a-8$$



$$\alpha = \frac{B_0}{\sqrt{\mu \rho g a}} \quad 3a-9$$

$$R = \alpha^2 Rm \quad 3a-10$$

We have nondimensionalized with the density  $\rho$ , the acceleration due to gravity  $g$ , the inner radius of the solenoid  $a$ , the magnetic permeability  $\mu$ , the conductivity  $\sigma$ , and the initial magnetic field  $B_0$ , due to  $I_0$ . As discussed in the Introduction, we consider an inviscid, incompressible fluid without surface tension.  $Rm$  is the magnetic Reynolds number,  $\alpha$  the Alfvén number.

We linearize with the small parameter

$$\epsilon = \frac{I_0 - i_1}{I_0} \quad 3a-11$$

Then

$$\vec{b} = \vec{1}_z + \vec{b} \quad 3a-12$$

and  $\vec{b}$ ,  $\vec{j}$ ,  $\vec{e}$ ,  $\vec{v}$  are considered of order  $O(\epsilon)$ .

As discussed in Section III, we consider the limit process  $Rm \rightarrow 0$ ,  $\alpha^2 Rm \rightarrow 1$ , applied to the linearized equations. First, we consider the equations and boundary conditions on the magnetic field.

For either  $z \gtrless 0$ , as  $Rm \rightarrow 0$ , we have

$$\text{div } \vec{b} = 0 \quad 3a-13$$

$$\text{curl } \vec{b} = 0 \quad 3a-14$$

and at  $z = \pm \infty$ ,  $r < 1$ ;

$$\vec{b} = \vec{1}_z b_z, \quad 3a-15$$

where  $b_z(t)$  is the perturbation field due to the change in solenoid current. Since  $\vec{b}$  is continuous at  $z = 0$ , and harmonic for all  $z$ , it follows that

$$\begin{aligned}\vec{b} &= \vec{I}_z b_z(t), \quad r < 1, \quad \text{all } z \\ \vec{b} &= 0, \quad r > 1, \quad \text{all } z\end{aligned}\tag{3a-16}$$

The complexity of the magnetic boundary conditions in the solenoid problem with finite  $Rm$  was discussed in the Introduction. The great simplification (Eq. 3a-16) here is due to the limit  $Rm \rightarrow 0$ .

In Sections IV and V, we derived the governing equation for the pressure as  $Rm \rightarrow 0$ ,  $R$  fixed.

$$\frac{\partial}{\partial t} \nabla^2 p + R \frac{\partial^2 p}{\partial z^2} = -R \frac{d^2 b_z}{dt^2}; \quad R = \alpha^2 Rm \tag{3a-17}$$

Equation 3a-18 is a consequence of equation 3a-16, the continuity and momentum equations.

Consider the nondimensional surface to be

$$\zeta(r, t) - z = 0 \tag{3a-18}$$

Then, at the surface, the fluid pressure is zero, hence

$$p(r, \zeta, t) = 0 \tag{3a-19}$$

and no fluid flows through the surface;

$$\frac{\partial^2 \zeta}{\partial t^2} = \left( -\frac{\partial p}{\partial z} - 1 \right)_{(r, \zeta, t)} \tag{3a-20}$$

At the wall of the solenoid, the radial velocity must be zero; this

means that

$$\left. \frac{\partial p}{\partial r} \right)_{r=1, z < 0, t=0} \quad 3a-21$$

Far below the surface, the effects of the surface die out, while the effects of the changing magnetic field, and hydrostatic pressure remain. Hence, as  $z \rightarrow -\infty$

$$p \rightarrow f(r, t) - z \quad 3a-22$$

With a given  $\frac{db_z}{dt}$ , equations 3a-17 to 3a-22 pose an initial value problem. We proceed as follows: as  $z \rightarrow -\infty$ , using equation 3a-22, we find the equation for  $p$  to be

$$\frac{\partial}{\partial t} \frac{1}{r} \frac{\partial}{\partial r} r \frac{\partial}{\partial r} p = -R \frac{d^2 b_z}{dt^2} \quad 3a-23$$

Hence  $p$  may be written as

$$p = \phi - z - \frac{r^2}{4} R \frac{d}{dt} b_z(t) \quad 3a-24$$

where  $p \rightarrow f(t)$  as  $z \rightarrow -\infty$ .  $\phi$  satisfies

$$\frac{\partial}{\partial t} \nabla^2 \phi + R \frac{\partial^2 \phi}{\partial z^2} = 0 \quad 3a-25$$

Next, we introduce the Laplace transform:

$$\bar{p}(r, z, s) = \int_0^{\infty} e^{-st} p(r, z, t) dt \quad 3a-26$$

$$p(r, z, t) = \frac{1}{2\pi i} \int_{-i\infty}^{i\infty} e^{st} \bar{p}(r, z, s) ds$$

Applying the transform, we find

$$\bar{p} = \bar{\phi} - z - \frac{r^2}{4} R \frac{d\bar{b}_z}{dt} \quad 3a-27$$

where  $\bar{\phi} = f(s)$  as  $z \rightarrow -\infty$ ; and  $\bar{\phi}$  satisfies

$$s \frac{1}{r} \frac{\partial}{\partial r} r \frac{\partial}{\partial r} \bar{\phi} + \frac{\partial^2}{\partial z^2} \bar{\phi} + R \frac{\partial^2}{\partial z^2} \bar{\phi} = 0 \quad 3a-28$$

The boundary conditions become

$$\left. \frac{\partial \bar{p}}{\partial r} \right|_{r=1, z, s} = 0 \quad 3a-29$$

$$\bar{p}(r, \bar{\zeta}, s) = 0 \quad 3a-30$$

$$s \frac{\partial^2}{\partial \bar{\zeta}^2} (r, s) = \left( -\frac{\partial \bar{p}}{\partial z} - 1 \right)_{(r, \bar{\zeta}, s)} \quad 3a-31$$

To satisfy 3a-29, we expand  $\bar{\phi}$  and  $\bar{p}$  in Dini Series (see Watson, Ref. 2).

Then  $\bar{\phi}$  is

$$\bar{\phi} = \sum_{m=0}^{\infty} f_m(z, s) J_0(k_m r) ; \quad J_1(k_m) = 0. \quad 3a-34$$

The  $f_m$  satisfy

$$f_0 = f(s) \quad 3a-35$$

$$\frac{\partial^2}{\partial z^2} f_m - \frac{k_m^2}{R+s} f_m = 0$$

The appropriate solution is

$$\bar{\phi} = \bar{C}_0(s) + \sum_{m=1}^{\infty} \bar{C}_m(s) \exp\left(z k_m \sqrt{\frac{s}{R+s}}\right) J_0(k_m r) \quad 3a-36$$

To find the correct expansion for  $\bar{p}$ , we use the Dini series expansion for  $r^2$ :

$$r^2 = \frac{z}{3} + 4 \sum_{m=1}^{\infty} \frac{J_0(k_m r)}{k_m^2 J_0(k_m)} ; J_1(k_m) = 0 \quad 3a-37$$

Hence we find the representation for  $\bar{p}$  to be

$$\bar{p} = \bar{C}_0 + \sum_{m=1}^{\infty} \bar{C}_m(s) \exp\left(z k_m \sqrt{\frac{s}{R+s}}\right) J_0(k_m r) - \frac{R}{4} \frac{d\bar{b}_z}{dt} \left( \frac{z}{3} + 4 \sum_{m=1}^{\infty} \frac{J_0(k_m r)}{k_m^2 J_0(k_m)} \right) - z \quad 3a-38$$

Equation 3a-38 satisfies the boundary conditions at  $r = 1$ ,  $z < 0$ ; and at  $z = -\infty$ ,  $r < 1$ . There remain the boundary conditions at the free surface. In view of the form of equation 3a-38, we expand  $\zeta$  in a Dini series also:

$$\bar{h} = \sum_{m=1}^{\infty} \bar{E}_m(s) J_0(k_m r) ; J_1(k_m) = 0 \quad 3a-39$$

Because

$$\int_0^1 \bar{h}(r, s) r dr = 0 = \bar{E}_0(s)$$

3a-39 is summed from  $m = 1$ .

Using equations 3a-38 and 3s-39, and equations 3a-30 and 3a-31, we find two algebraic equations which determine the  $\bar{C}_m$ ,  $\bar{E}_m$ . They are

$$\left\{ \bar{C}_0 - \frac{R}{6} \left( \frac{d\bar{b}_z}{dt} \right) \right\} + \bar{C}_m - R \left( \frac{d\bar{b}_z}{dt} \right) \frac{1}{k_m^2 J_0(k_m)} - E_m = 0 \quad 3a-40$$

and

$$- \bar{C}_m(s) k_m \sqrt{\frac{s}{R+s}} = s^2 \bar{E}_m \quad 3a-41$$

To obtain equations 3a-40 and 3a-41, we substitute  $\bar{\zeta}$  into equations 3a-30 and 3a-31 and expand the exponentials in  $k_m \bar{\zeta} \frac{s}{R+s}$ , keeping only the first terms.

Solving, we find

$$\bar{C}_0 = \frac{R}{6} \left( \frac{d\bar{b}_z}{dt} \right) \quad 3a-42$$

and

$$\bar{h}(r, s) = - \sum_{m=1}^{\infty} \frac{R \left( \frac{d\bar{b}_z}{dt} \right) J_0(k_m r)}{\left( 1 + \frac{s^2}{k_m^2} \sqrt{\frac{R+s}{s}} \right) k_m^2 J_0(k_m)} \quad 3a-43$$

Hence we obtain the following expression for  $\zeta$  :

$$h(r, t) = - \sum_{m=1}^{\infty} \frac{R J_0(k_m r)}{k_m^2 J_0(k_m)} \frac{1}{2\pi i} \int_{-i\infty}^{i\infty} \frac{e^{st}}{1 + \frac{s^2}{k_m^2} \sqrt{\frac{R+s}{s}}} \frac{d\bar{b}_z}{dt} ds \quad 3a-44$$

As in Appendix I and Appendix II, the branch cuts lie along the negative real  $s$  axis and go from  $s = -R$  and  $s = 0$ , to  $s = -\infty$ .

With this choice of cuts, the integral

$$P = \frac{1}{2\pi i} \int_{-i\infty}^{i\infty} e^{st} \bar{p}(s) ds$$

exists. To eliminate  $R$  from the integral in 3a-44, we introduce new variables (see Appendix II)

$$\begin{aligned} s^* &= \frac{s}{R} & 3a-45 \\ t^* &= Rt \\ k_m^* &= k_m / R^2 \end{aligned}$$

Then the integral in equation 3a-44 becomes

$$\frac{-R^2}{2\pi i} \int_{-i\infty}^{i\infty} \frac{e^{s^* t^*}}{1 + \frac{s^{*2}}{k_m^*} \sqrt{\frac{1+s^*}{s^*}}} \overline{db_z^*} ds^* = \ell_m(t^*) \quad 3a-46$$

Consider first  $\frac{d}{dt^*} b_z(t^*) = 1$ , i. e.  $\frac{d}{dt^*} b_z(t^*) = \delta(t^*)$ . Then we have to consider

$$\frac{R^2}{2\pi i} \int_{-i\infty}^{i\infty} \frac{e^{s^* t^*} ds^*}{1 + \frac{s^{*2}}{k_m^*} \sqrt{\frac{1+s^*}{s^*}}} \quad 3a-47$$

Now the function

$$k_m^* + s^{*2} \sqrt{\frac{1+s^*}{s^*}}$$

has two zeros, of the form (see Appendix II)

$$s^* = -\gamma(k_m^*) \pm i\omega(k_m^*) \quad 3a-48$$

Where  $\gamma, \omega > 0$ . The contour integration of 3a-47 thus yields

$$\frac{R^2 k_m^*}{\omega(k_m^*)} e^{-\gamma(k_m^*)t^*} \cos(\omega t^* - \frac{\pi}{2}) + Q(k_m^*, t^*) \quad 3a-49$$

where  $Q(k_m^*, t^*)$  is the result of integration around the branch cuts.

$$Q(k_m^*, t^*) = \frac{R^2 k_m^*}{\pi} \int_0^1 \frac{e^{-\eta t^*} \eta^2 \sqrt{\frac{1-\eta}{\eta}}}{k_m^{*2} + \eta^3(1-\eta)} d\eta \quad 3a-50$$

The general solution for arbitrary  $b_z(t)$  is obtained by forming the convolution integral:

$$l_m(t^*) = -R^2 k_m^* \int_0^{t^*} \frac{db_z(t^*-s)}{dt^*} \left\{ \frac{e^{-\gamma s}}{\omega} \cos(\omega s - \frac{\pi}{2}) + \frac{Q}{R^2 k_m^*} \right\} ds \quad 3a-51$$

Now consider the term in brackets as  $R \rightarrow 0$ : as  $R \rightarrow 0$ ,  $k_m^* \rightarrow \infty$ , and  $Q \rightarrow 0$ . Further  $-\gamma \rightarrow \frac{1}{4}$ ,  $\omega \rightarrow \sqrt{k_m^* - \frac{3}{16}}$ . Hence equation 3a-51 becomes

$$l_m(t^*) = \frac{-R^2 k_m^*}{\sqrt{k_m^* - \frac{3}{16}}} \int_0^{t^*} \frac{db_z(t^*-s)}{dt^*} \left\{ e^{-\frac{1}{4}s} \cos(\sqrt{k_m^* - \frac{3}{16}} s - \frac{\pi}{2}) \right\} ds \quad 3a-52$$



Since a term inside the brackets like  $\cos(\sqrt{k_m^*} s - \frac{\pi}{2})$  would denote the response of the  $m^{\text{th}}$  gravity mode of surface oscillations, we see that the first term in the brackets of equation 3a-52 is the  $m^{\text{th}}$  damped normal mode of the system. Thus, in equation 3a-51, this term is the response of the  $m^{\text{th}}$  damped normal mode of the surface, analogous to the gravity mode  $\cos(\sqrt{k_m^*} t^* - \frac{\pi}{2})$  when  $R = 0$ . The second term in the brackets is, for large  $t^*$ , monotonic decreasing to zero in  $t^*$ , for non-oscillatory  $b_z(t^*)$ . It is due to the Alfvén wave structure in the problem.

In general, the surface shape is given by

$$h(r, t) = \sum_{m=1}^{\infty} \frac{l_m(t^*) R J_0(k_m r)}{k_m^2 J_0(k_m)} \quad 3a-53$$

where  $l_m(t^*)$  is given by 3a-51. This completes the theoretical solution to the solenoid problem.

## APPENDIX IV

## EXPERIMENTS

## A. Introduction

The experiments used mercury as the conducting fluid; the conductivity of mercury is  $\sigma = 1.04 \times 10^8$  mhos/meter. The permeability of mercury is very nearly that of free space. The solenoid is 1 meter high with an ID of 15 cm. This gives a magnetic Reynolds number of  $R_m = \mu\sigma a\sqrt{ag} = .08$ . The mercury filled the solenoid to a depth of about 70 cm. The surface motion was measured with graphite pencil lead resistors, and the magnet current was read from a shunt. The surface deflection at four points and the magnet current were recorded on oscilloscope photographs.

The probes used to measure the surface deflection consisted of three joined pieces of TEC 5H drafting leads. The joints were made by making a tight coil of tinned soft copper wire over a number 46 drill, then removing the drill, sliding the lead ends to be joined into the coil, and soldering the joint with the leads aligned. Finally, the joints were coated with spoxy for insulation. In this way, we were able to construct graphite rods of about  $100 \Omega$  resistance which were 15 inches long, .077 inches in diameter, and parallel to within  $\frac{1}{64}$  inches. When such a rod has one end grounded in the mercury, its resistance was found to change linearly and repeatably (within 1 per cent) as the depth of the lead in the mercury changed. From this change in resistance a voltage

was produced which was recorded by an oscilloscope. Figure 1 shows the circuit.

The frequency response of the probes was estimated as higher than 1000 cycles/sec. The major error in such a transducer comes from the trace width on the oscilloscope, and from the induction effects of the probe as it responds to the changing magnetic field. The latter effects were of significance for short times only, and calibrated corrections were obtained by repeating the experiments with the Battery E (see Fig. 1) disconnected. The probes were aligned to the centerline of the solenoid to within about  $\frac{1}{16}$  inch. Figure 2 shows the arrangement of mounting the probes. Radial symmetry of the surface motion was observed visually, hence the probes were placed in one plane for convenience. The spacing is shown in Figure 2.

The magnet circuit is shown in Figure 3; the voltage across a calibrated shunt (30 mv at 1500 amps) was recorded to give the magnetic current. A 250 cycle filter was used to remove the high frequency noise of the MG set, which was in poor condition at the time of the experiments. At the beginning and end of each run, the initial and final current was read from the ammeter on the control panel of the MG set. Since the magnetic field in the solenoid was calibrated with this meter, the initial and final values of the field in the solenoid were known to within 1 per cent.

With this equipment, to produce a  $\frac{db}{dt}$  large enough to have measurable surface wave amplitudes, it is necessary to switch on or off the MG set. This produces an exponentially rising or decaying

magnetic field.

However, there is no doubt that hydromagnetic surface waves exist when formed by a small change in current. If the magnet current is raised slowly, and if a small sudden change in current occurs, a ripple is visually observed on the mercury surface. The amplitude of such a disturbance is very small.

Experiments were done with initial or final field strengths from 2000 to 10000 gauss; below 4000 gauss the amplitude of the surface motion was too small to record accurately. Above from 9000 gauss it was thought that the impulsive loading or unloading could damage the MG set, so only exploratory data were obtained in this region.

## B. Description of the Data

Six experiments were analyzed in detail. These consisted of the response of the surface due to the exponentially rising or decaying magnetic field, for three values of the initial or final field strength. The magnetic field strength varied between 4000 and 9000 gauss. Exploratory runs for higher and lower field strengths were also obtained; but all features of the latter data appear in the six runs mentioned above. The description of the data includes a graphical representation of the surface motion, and a discussion of the magnet current and magnetic field.

From measuring the magnetic field directly with a coil inside the large magnet connected through an integrating circuit to an oscilloscope, we find that when the magnet is switched off, the field decays exponentially with a half time of  $0.045 \pm 0.002$  sec. When the current is switched on, the field rises exponentially as  $\{1 - \exp(-\lambda t)\}$ , and the half time for this rise is  $0.119 \pm 0.001$  sec. Comparing the field when the solenoid is filled with mercury, and empty, we find that the presence of the mercury does not change the magnetic field.

Due to a ground shift as the magnet is switched on and off, the current traces show an initial rise or fall of about 30 per cent. However, the decay times agree: for switching off, the half time found from the current traces is  $0.47 \pm 0.003$  sec, and for switching on,  $0.11 \pm 0.001$  sec. The switching on rise time is a property of the MG set; the decay time, a property of the magnetic switching circuit (which agrees with the calculated decay time for the magnet circuit).

When the magnet current is switched off, the maximum surface deflection occurs in the center of the tank at .20 sec after the switching process. The maximum is followed by damped, roughly sinusoidal oscillations. The amplitude of the maximum deflection increases steadily as the initial field strength increases, until an amplitude of nearly 5 cm is reached, at which time the maximum has become a sharp, rather than a sinusoidal rounded peak, indicating the presence of nonlinear effects. At the time of the first maximum, the magnetic field has decayed to about 6 per cent of its initial value. See Figures 4, 5, and 6.

When the magnet current is switched on, the maximum amplitude is about .20 cm; it occurs about .20 sec after the switching process. The oscillations following the first maximum are strongly damped. As the final field strength increases, the damping increases, with the higher field strengths producing over-critical damping. At the lowest field strength for which the amplitude of the surface motion was measurable, the center region of the surface made one complete cycle before being damped. The best sensitivity of the surface probes with maximum available amplification is about .02 cm in the absence of induction corrections and noise. Hence the data for switching on the magnet are not very accurate. See Figures 7, 8, and 9.

In both cases of switching off and on, the induction corrections were large at time  $t = 0$ ; the corrected value of the surface deflection being the difference between two large numbers. Hence the initial part of the surface motion has a large error. This error is negligible after about .20 sec in all cases. The noise is represented on the graphs as the trace width; generally  $\frac{1}{5}$  of the trace width would be a fair estimate of the error due to noise.

### C. Comparison of Theory and Experiment

In this section we shall use the theory derived in Appendix III as a description of the phenomena observed in the experiment. However, since the experimental surface oscillations were caused by an exponentially rising or falling magnetic field, we first must decide which conditions we shall linearize about, in order to apply the linearized theory of Appendix III. We choose to linearize about the initial magnetic field strength for the switching off experiments; and the final magnetic field strength for the switching on experiments. Hence  $B_0$  is the non-zero initial or final magnetic field in the switching process. With this choice, the only formal difference between the equation for the surface deflection in the switching off and on cases is a change in sign, and the half time for the switching process.

Next, we wish to find a simple approximation to equations 3a-51 and 3a-53. We proceed as follows: For the six runs described in the previous section, with the linearization described above,  $R$  varies between one and five. The dominant term in  $\zeta(r, t)$  is the one due to the lowest eigen value,  $k_1$ . All other terms may be considered as corrections to this one. Since  $k_1 \approx 3.84$ , for the six runs in question,  $k_1^* = k_1/R^2$  varies between  $\frac{1}{10} < k_1^* < 3.8$ . We desire approximations in this range of  $k_1^*$ . We shall consider only the term due to  $k_1$  in  $\zeta(r, t)$ . Now in this term, the second term in the brackets of equation 3a-51 is

$$\int_0^{t^*} \frac{db_z}{dt^*} (t^* - s) Q(s; k_1^*) ds$$

Now  $Q(s)$  is monotonic decreasing with increasing  $s$ . Hence for exponential  $b_z(t^*)$  this term has at most one maximum, and is non-oscillatory. Since we are interested mainly in the character of the surface oscillations, we ignore this term in  $Q$ . Thus we get the following approximation to the surface motion:

$$\zeta(r, t^*) = \frac{-R^3 k_1^* J_0(k_1 r)}{k_1^2 J_0(k_1)} \int_0^{t^*} \frac{db_z(t^*-s)}{dt^*} \left\{ \frac{e^{-\gamma s}}{\omega} \cos(\omega s - \frac{\pi}{2}) \right\} ds \quad 4a-1$$

where  $J_0$  is the Bessel function of the first kind, of order zero;  $\gamma$  and  $\omega$  are the real and imaginary parts of the zeros of

$$k_1^{*2} + s^2 \sqrt{\frac{1+s}{s}} = 0 \quad ; \quad s = -\gamma \pm i\omega \quad 4a-2$$

the physical time  $T$  is

$$T = \sqrt{\frac{a}{g}} \frac{t^*}{R} \quad 4a-3$$

$r$  is the nondimensional cylinder radius; and

$$\frac{db_z}{dt^*} = \pm \lambda^* \exp(-\lambda^* t^*) \quad 4a-4$$

where

$$\lambda^* = \sqrt{\frac{a}{g}} \frac{\log 2}{R \tau} \quad 4a-5$$



In equation 4a-4, the plus sign describes the switching on process and the minus sign the switching off process. In equation 4a-5,  $\tau$  is the appropriate half time for the switching process.  $R$  is, of course

$$R = \alpha^2 R_m = \frac{\sigma B_0^2}{g} \sqrt{\frac{a}{g}} \quad 4a-6$$

For  $k_1^* \gg \frac{3}{10}$  an approximation to  $\gamma, \omega$  is

$$s = -\frac{1}{4} \pm i \sqrt{k_1^* - \frac{3}{16}} \quad 4a-7$$

Here,  $R$  must be smaller than

$$R < \sqrt{\frac{10}{3}} (3.84) \approx 3.5$$

This includes four out of the six runs.

Using equation 4a-7, we may integrate equation 4a-1 to find

$$h(r, t^*) = \pm \frac{R^3 k_1^* J_0(k_1 r) \left[ e^{-\lambda^* t^*} \sin \theta + e^{-\frac{1}{4} t^*} \sin \left[ \sqrt{k_1^* - \frac{3}{16}} t^* - \theta \right] \right]}{k_1^2 J_0(k_1) \sqrt{k_1^* - \frac{3}{16}} \sqrt{\left( \lambda^* - \frac{1}{4} \right)^2 + k_1^* - \frac{3}{16}}} \quad 4a-8$$

where

$$\theta = \tan^{-1} \left( \frac{\sqrt{k_1^* - \frac{3}{16}}}{\lambda^* - \frac{1}{4}} \right)$$

and the plus sign of equation 4a-8 refers to the switching off case, the minus sign to the switching on case.

For small field strengths,  $B_0$  is small, hence  $R$  is small, and  $k_1^*$  large. From equation 4a-8 we see that in this case, the amplitude of the oscillations increases as

$$\max \zeta(0, t^*) \sim \text{const} \times R^2 \lambda \sim \lambda B_0^4 \quad 4a-9$$

as  $B_0$  increases. As  $B_0$  increases, the frequency of oscillation

$$\omega = \sqrt{g/a} \sqrt{3.84 - \frac{3}{16} R^2} = \sqrt{\frac{gk_1}{a} - \frac{3}{16} \frac{\sigma^2 B_0^2}{\rho^2}} \quad 4a-10$$

decreases. The oscillations are damped as

$$- \frac{1}{4} R \sqrt{g/a} \sim - B_0^2 \quad 4a-11$$

as  $B_0$  increases. From equation 4a-9, we see that the amplitude increases as the half time of the switching process  $\tau \sim \frac{1}{\lambda}$  decreases.

Now consider Figure 10, a nondimensional plot of the experimental and theoretical results for  $\zeta(0, t^*)$ , for the switching off run at the (low) initial field strength of 4800 gauss. The theoretical curve was computed from equations 3a-51 and 3a-53 with no approximations. At the time of the first positive peak in  $\zeta(0, t^*)$ , the magnetic field has decayed to 6 per cent of its initial value.

For  $t^* < 2$ , the experimental data are inaccurate due to induction corrections.

Figure 11 shows a similar comparison for  $\zeta(0, t^*)$  for a switching on run. The final field strength is 4700 gauss. Here the theoretical amplitudes are far too large initially, due to the linearization about the final field strength. Notice that the theoretical amplitude is 10 times the experimental amplitude. The experimental amplitudes of the surface oscillations correspond roughly to a linearization about  $\frac{1}{2}$  the final field strength.

Finally, the fact that  $B$  was unchanged by the presence or absence of mercury in the solenoid indicates that the limit  $Rm \rightarrow 0$  and the resulting approximation  $B = B_z(t)$  are valid. Interactions with the changing field and surface motion are of a magnitude predicted by the theory when it was applicable. Hence holding  $\alpha^2 Rm \sim 1$  is also valid.

We conclude that the discrepancies between theory and experiment are due to the linearization.

However, the linearized theory contains qualitatively all the features of the experimental results.

To understand the above statements, we must modify the linearized theory to take into account the large changes in  $\alpha^2 Rm = R$ .  $\frac{dR(T)}{dT}$  is of the same size as  $\frac{db}{dt}$ . Hence we can not obtain a rigorously correct modification of the linearized theory by considering  $R(T)$  to vary "slowly" (compared to  $\frac{db}{dt}$ !) with time. Hence we seek an empirical modification of the linearized theory.

We argue as follows: At any time, the mercury in the solenoid

oscillates in a set of damped normal modes. We expect that the characteristics of these normal modes depend only on the instantaneous value of  $R$ . Thus the frequency, damping and phase of the first normal mode are given by

$$\omega = \sqrt{g/a} \sqrt{3.84 - \frac{3}{16} R^2(T)} \quad 4a-12$$

$$\gamma = -\frac{1}{4} R(T) \sqrt{g/a} \quad 4a-13$$

$$\theta = \tan^{-1} \left( \frac{\omega(T)}{\lambda - \gamma(T)} \right) \quad 4a-14$$

for  $R(T) < 3.5$ .  $\lambda$  is given by

$$\lambda = \frac{\log 2}{\tau} \quad 4a-15$$

where  $\tau$  is the half time of the switching process.

However, the amplitude at time  $T_0$  depends on the time history of the forcing function and the surface response for all times  $0 < T < T_0$ . Hence we may not in general compute the amplitude from the instantaneous value of  $R$ .

Denoting the amplitude of the first mode by  $A(T)$ , and using the above ideas, we write

$$l_1(T) = A(T) (e^{-\lambda T} \sin \theta + e^{-\gamma T} \sin(\omega T - \theta)) \quad 4a-16$$

where  $\gamma, \theta, \omega$  are now given by equations 4a-12 through 4a-14. Now we recognize that when  $R = 0$ , there is no coupling between the magnetic field and the surface motion. Hence

$$\frac{dA}{dT} = 0 \text{ for } R = 0 \quad 4a-17$$

Hence, for the switching off process

$$A \approx \text{const for } T > 2\tau \text{ say.}$$

4a-18

Computations, with  $A = \text{const}$ , for the switching off case, show that equation 4a-16 gives very nearly the correct phase and frequency up to  $T = .4 \text{ sec}$ ; this corresponds to  $t^* = 7$  in Figure 10.

We describe the small amplitudes of the switching on process by saying that  $A(T)$  rises very slowly from its zero value at  $T = 0$ . This is expected, for if  $A$  were given by the instantaneous value of  $R$ ,  $A \sim B^4$ .

## References

1. J. J. Stoker: Water Waves, Interscience Publishers, Inc., New York, 1957
2. G. N. Watson: Theory of Bessel Functions, second edition, The Macmillan Co., New York, 1948
3. H. W. Liepmann, D. P. Hoult and H. G. Ahlstrom: Concept, construction and preliminary use of a facility for experimental studies in magneto-fluid mechanics. Tollmien Festschrift, 1960
4. L. S. Solov'ev: Magneto-hydrodynamic Surface Waves, Soviet Physics, Vol. 6, No. 6, p. 294, October 1961
5. James R. Melcher: Electro-hydrodynamic and Magnetodynamic Surface Waves and Instabilities, Phys. Fluids, 4, 1348, 1961
6. L. E. Fraenkel: J. Fluid Mech. 1, (1960) 81
7. L. E. Fraenkel: Quart. J. Mech. and App. Math. 14 (1961) 173
8. S. Lundquist: Studies in MHD, Arkiv för Fysik, 5 (1952) 297

TABLE I

TABLE OF EXPERIMENTAL RUNS

Fig. No.	$\tau$ (sec)	Initial or Final Current (amps)	Initial or Final Field Strength $B_0$ (Webers/M <sup>2</sup> )	Switching
4	0.047	430	.4800	Off
5	0.047	600	.6700	Off
6	0.047	760	.8500	Off
7	0.11	422	.4700	On
8	0.11	630	.7000	On
9	0.11	840	.9400	On

$\zeta$  is non-dimensional surface shape at  $r=0$ .

The non-dimensional trace width is  $=0.04$ .

Times are in seconds  $\pm 0.005$ .

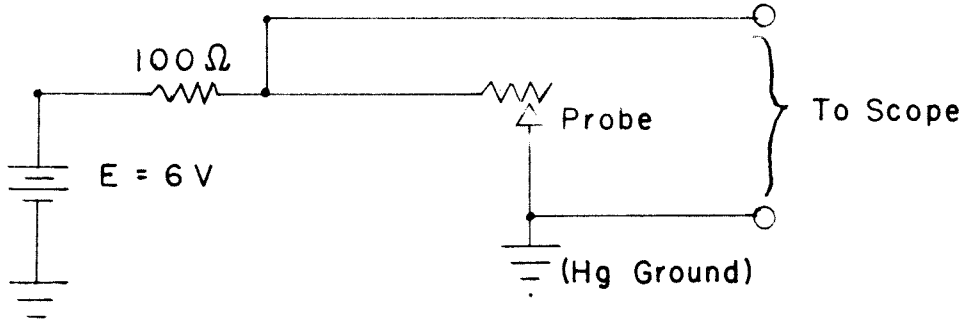


FIG. 1 PROBE CIRCUIT

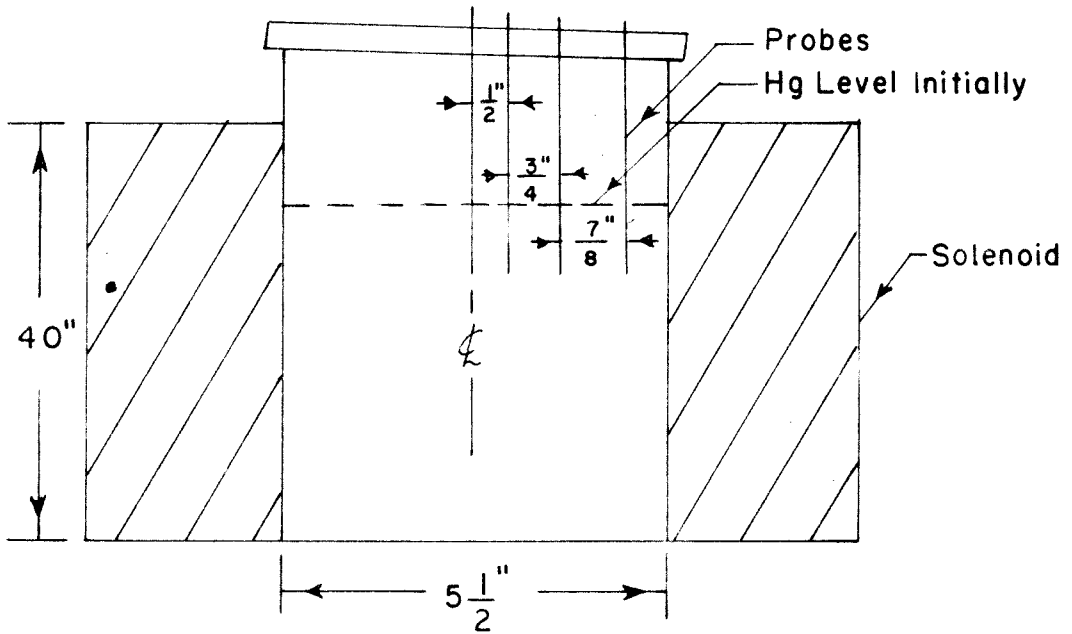


FIG. 2 PROBE SETUP

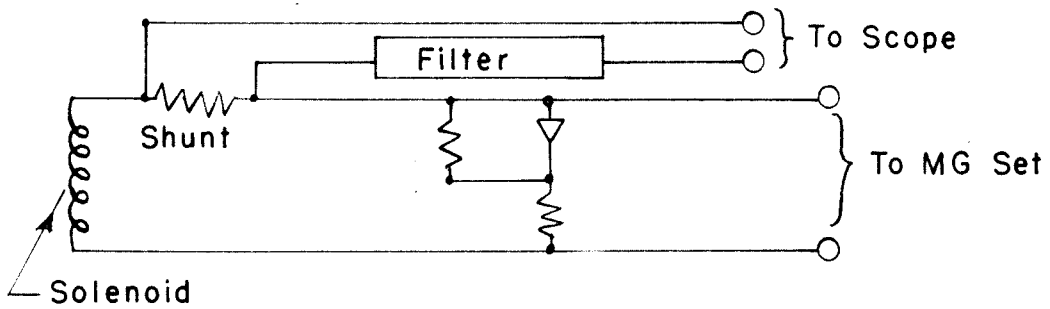
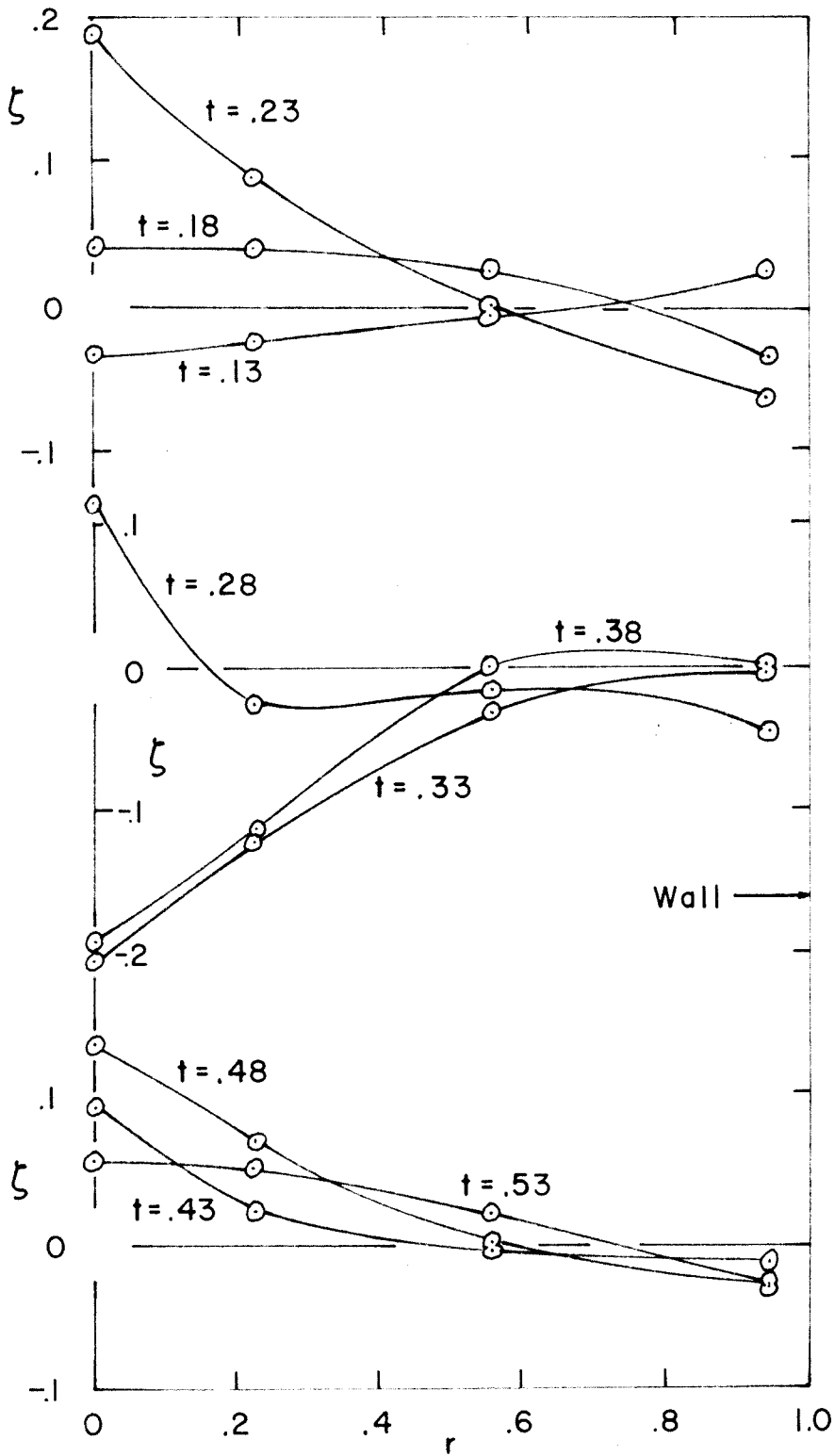


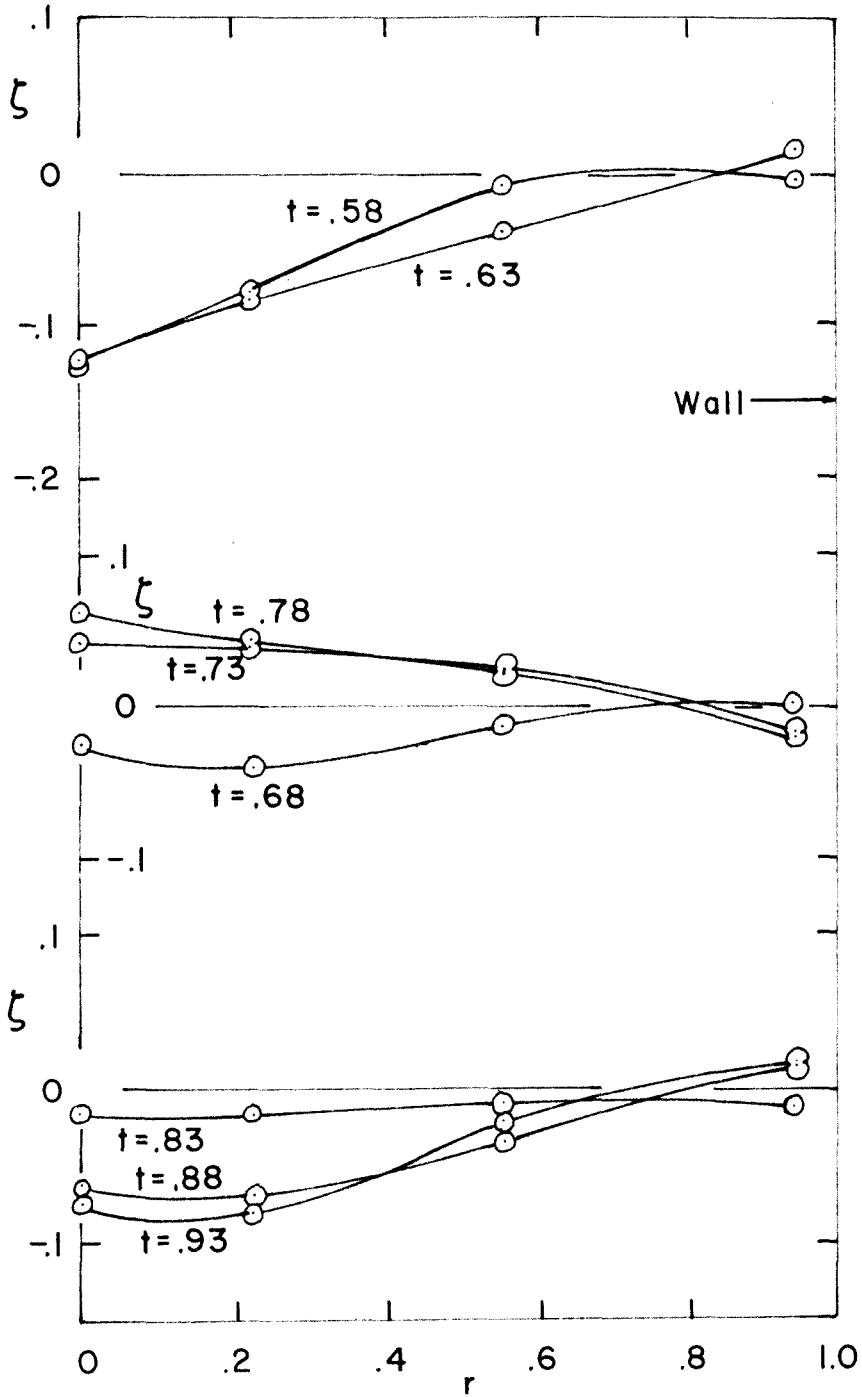
FIG. 3 MAGNET CIRCUIT



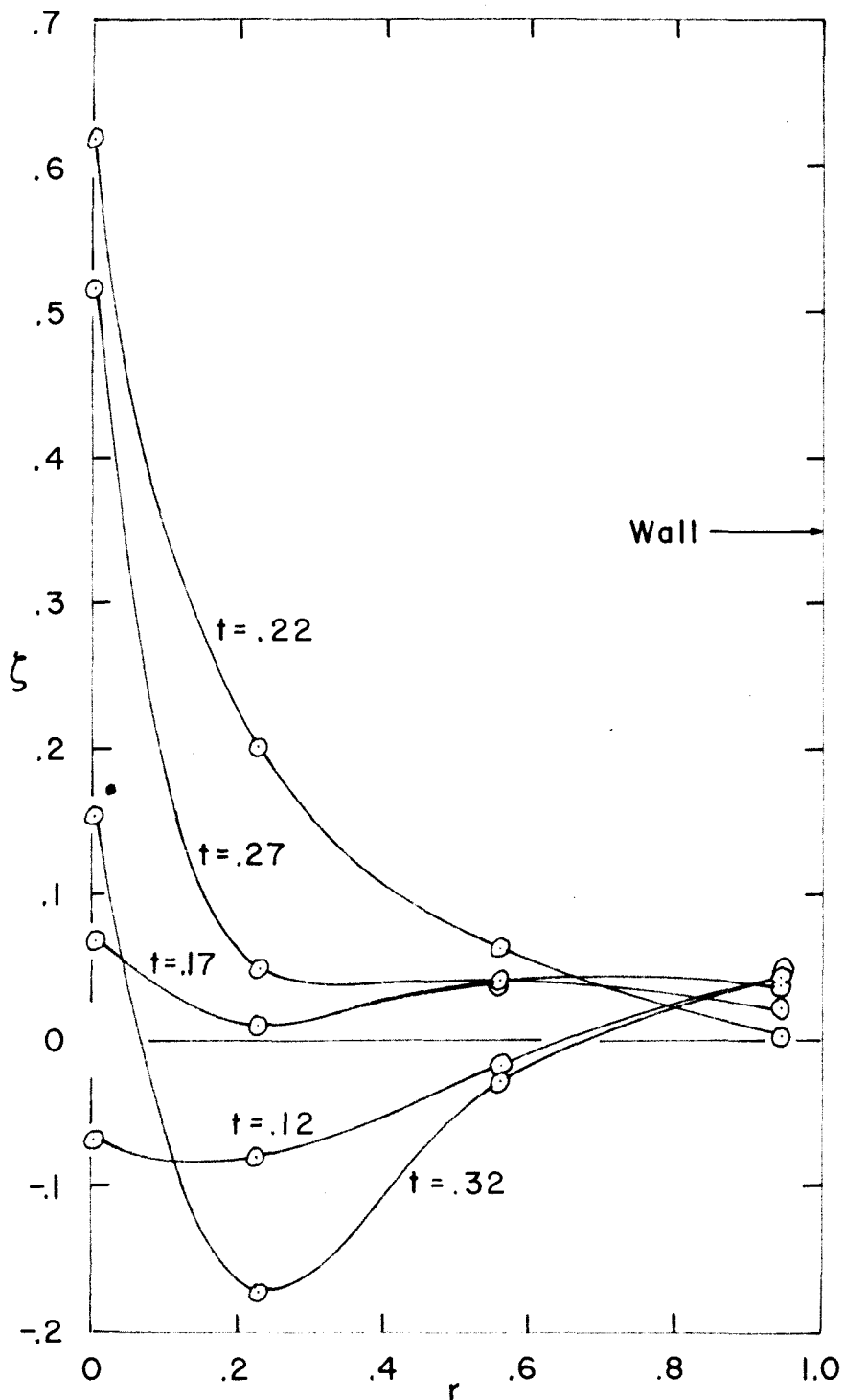


EXPERIMENTAL SURFACE DEFLECTIONS

FIG. 4a

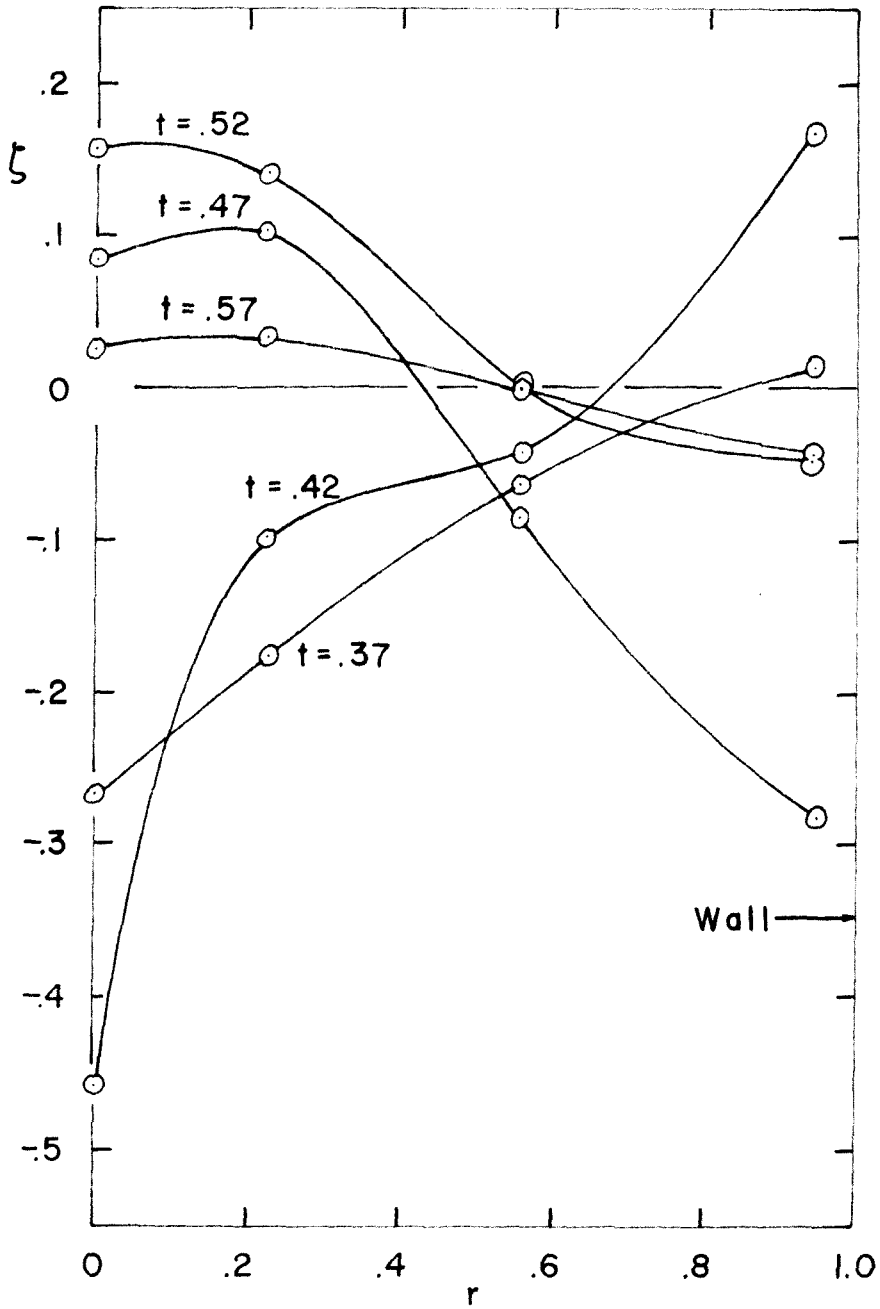


EXPERIMENTAL SURFACE DEFLECTIONS  
FIG. 4 b



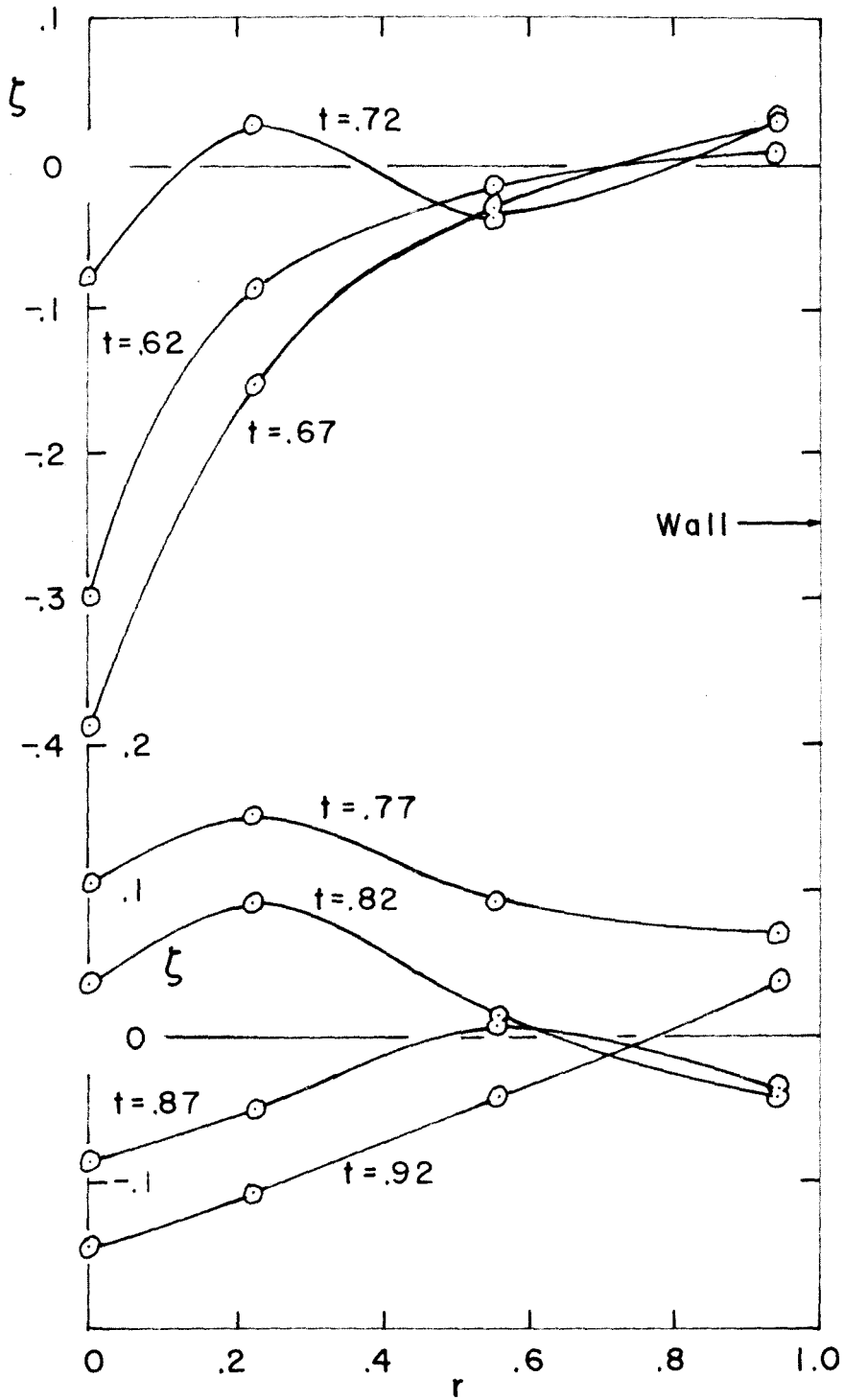
EXPERIMENTAL SURFACE DEFLECTIONS

FIG. 5a



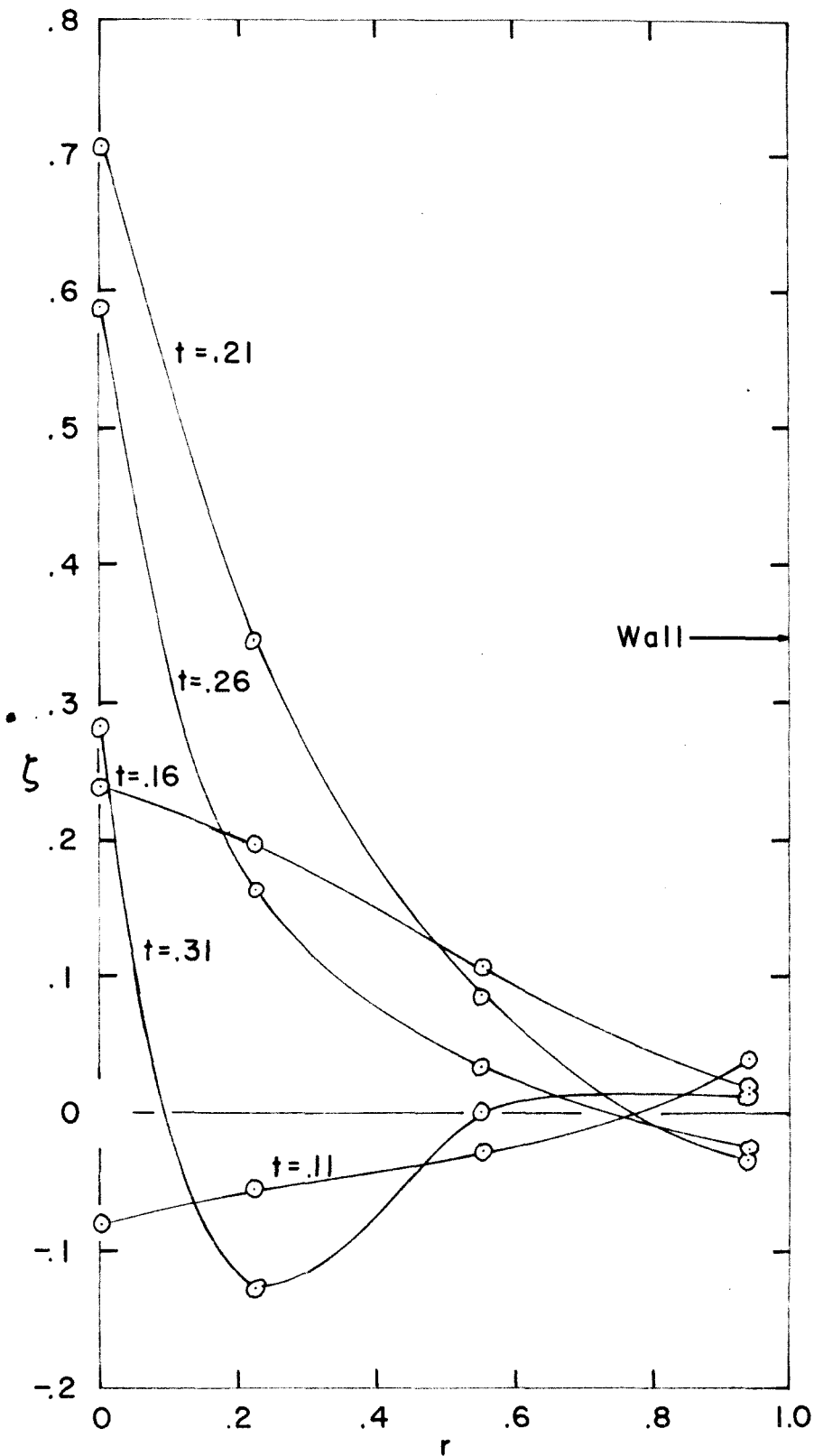
EXPERIMENTAL SURFACE DEFLECTIONS

FIG. 5 b

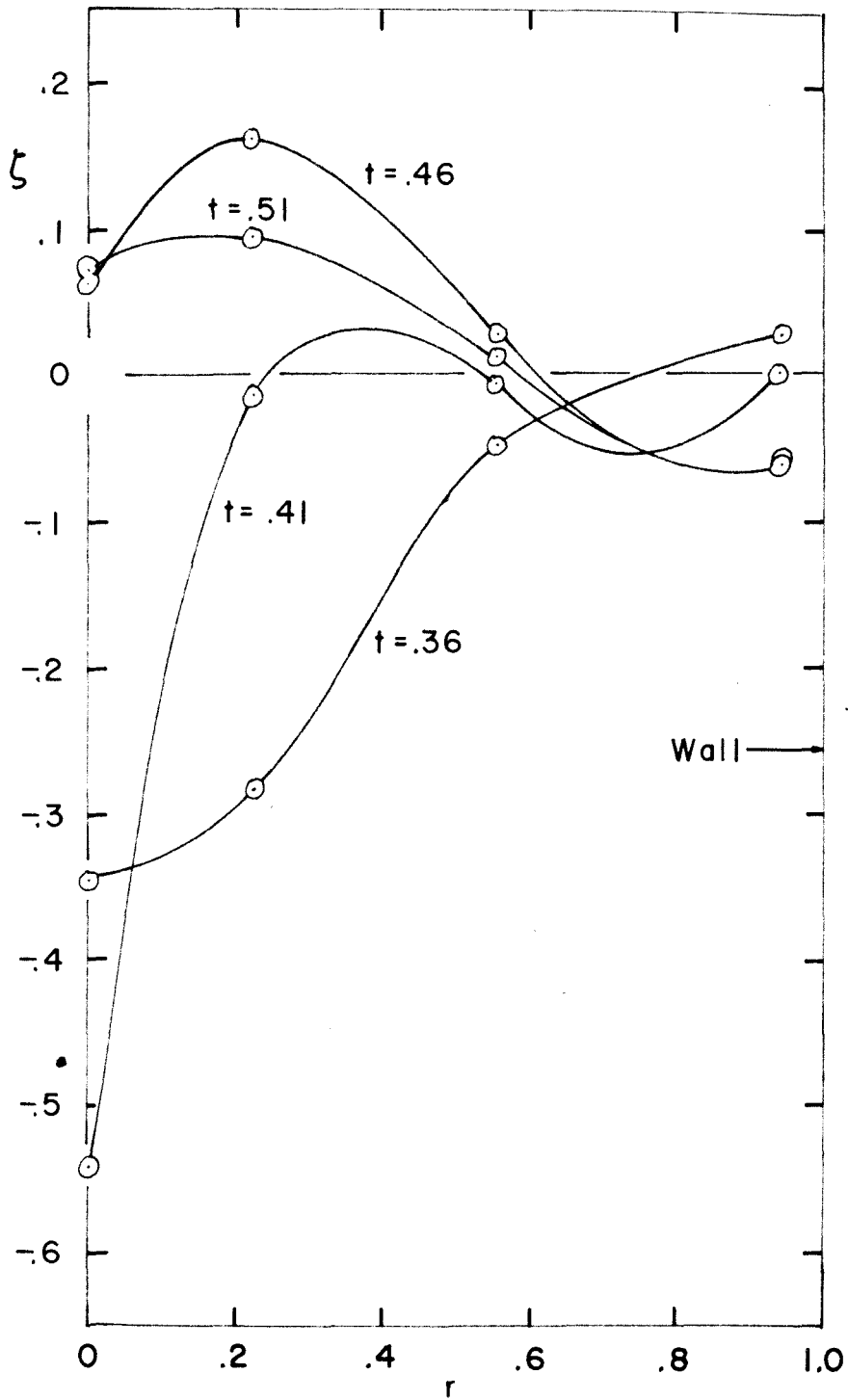


EXPERIMENTAL SURFACE DEFLECTIONS

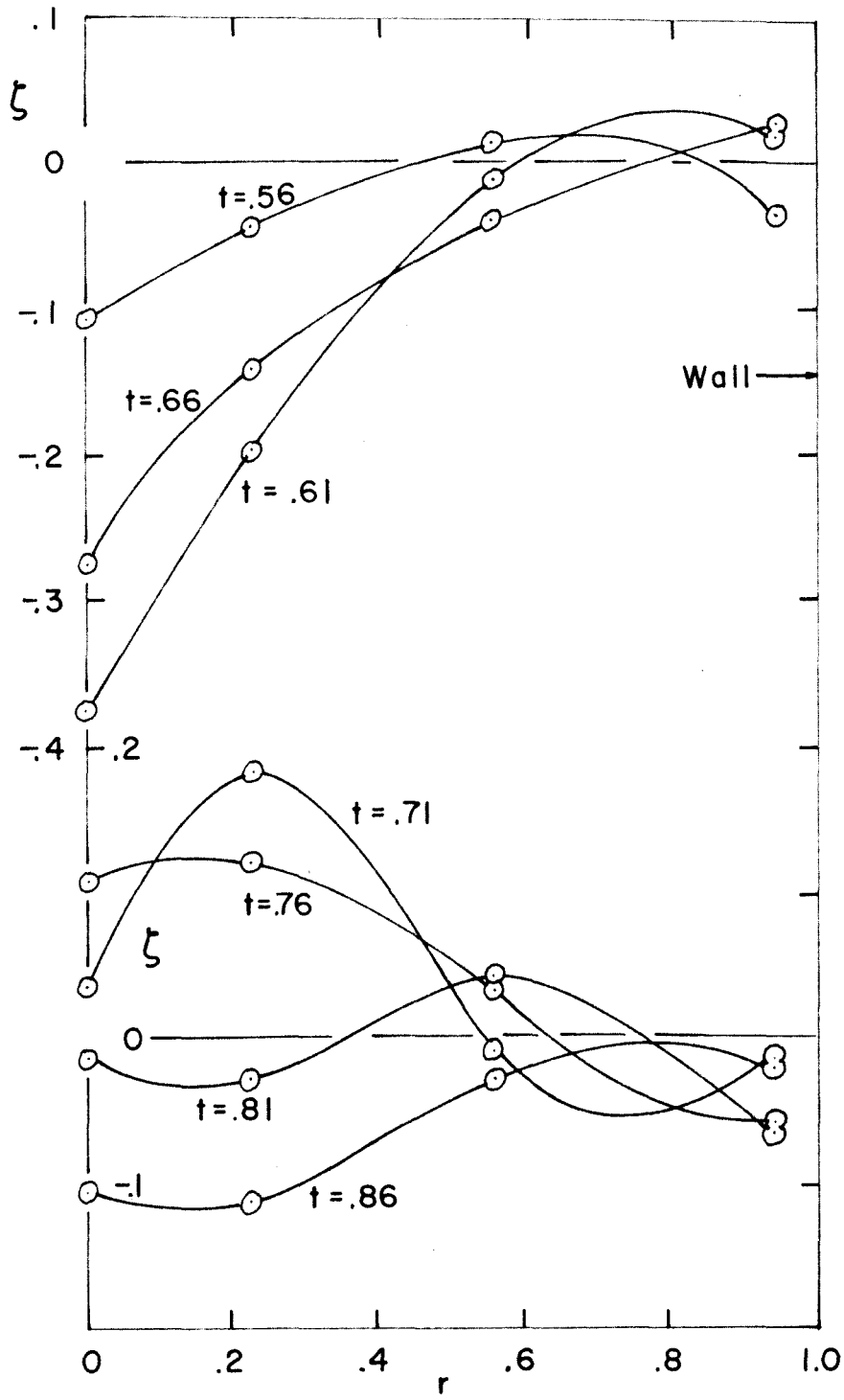
FIG. 5c



EXPERIMENTAL SURFACE DEFLECTIONS  
FIG. 6a

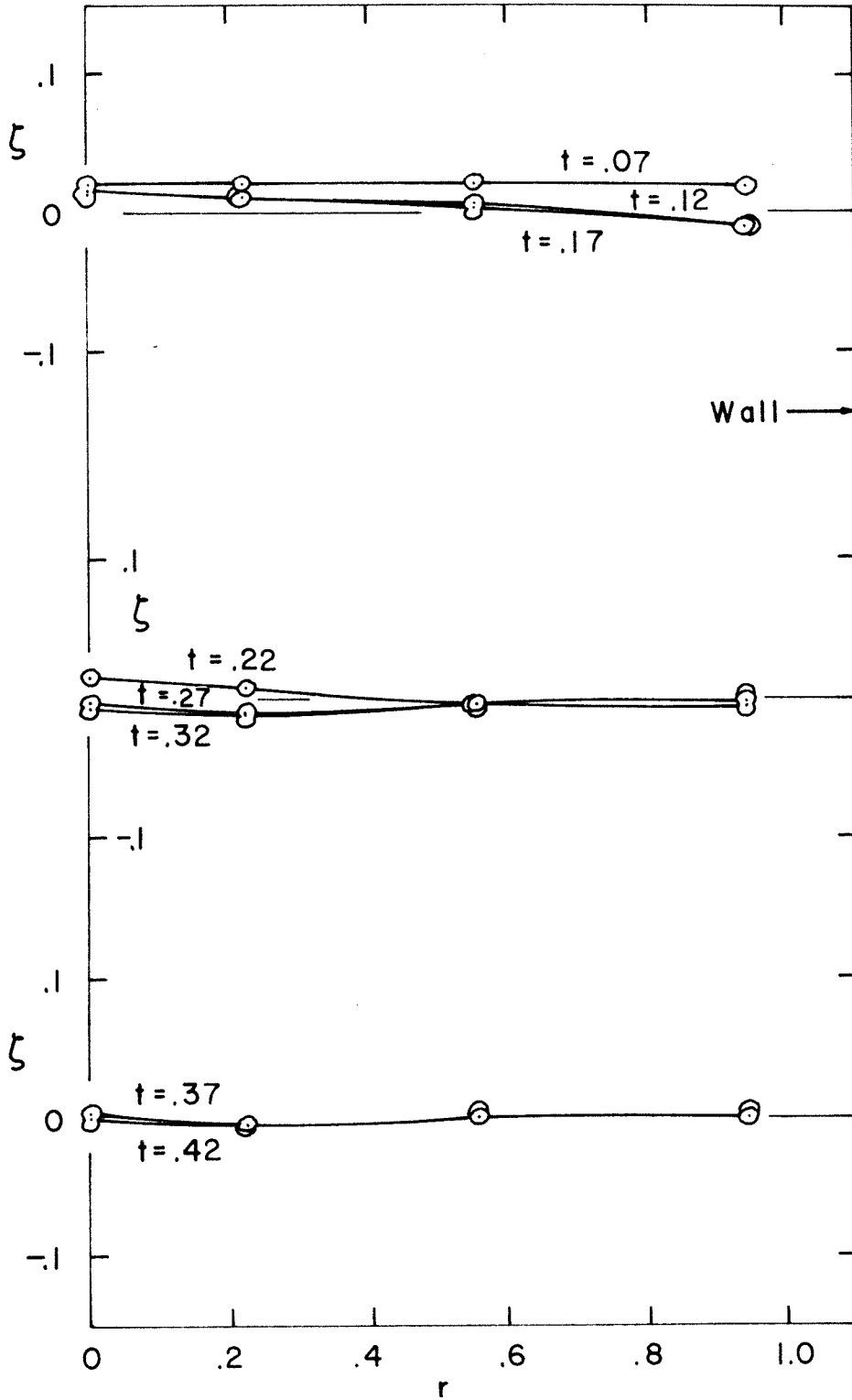


EXPERIMENTAL SURFACE DEFLECTIONS  
FIG. 6 b

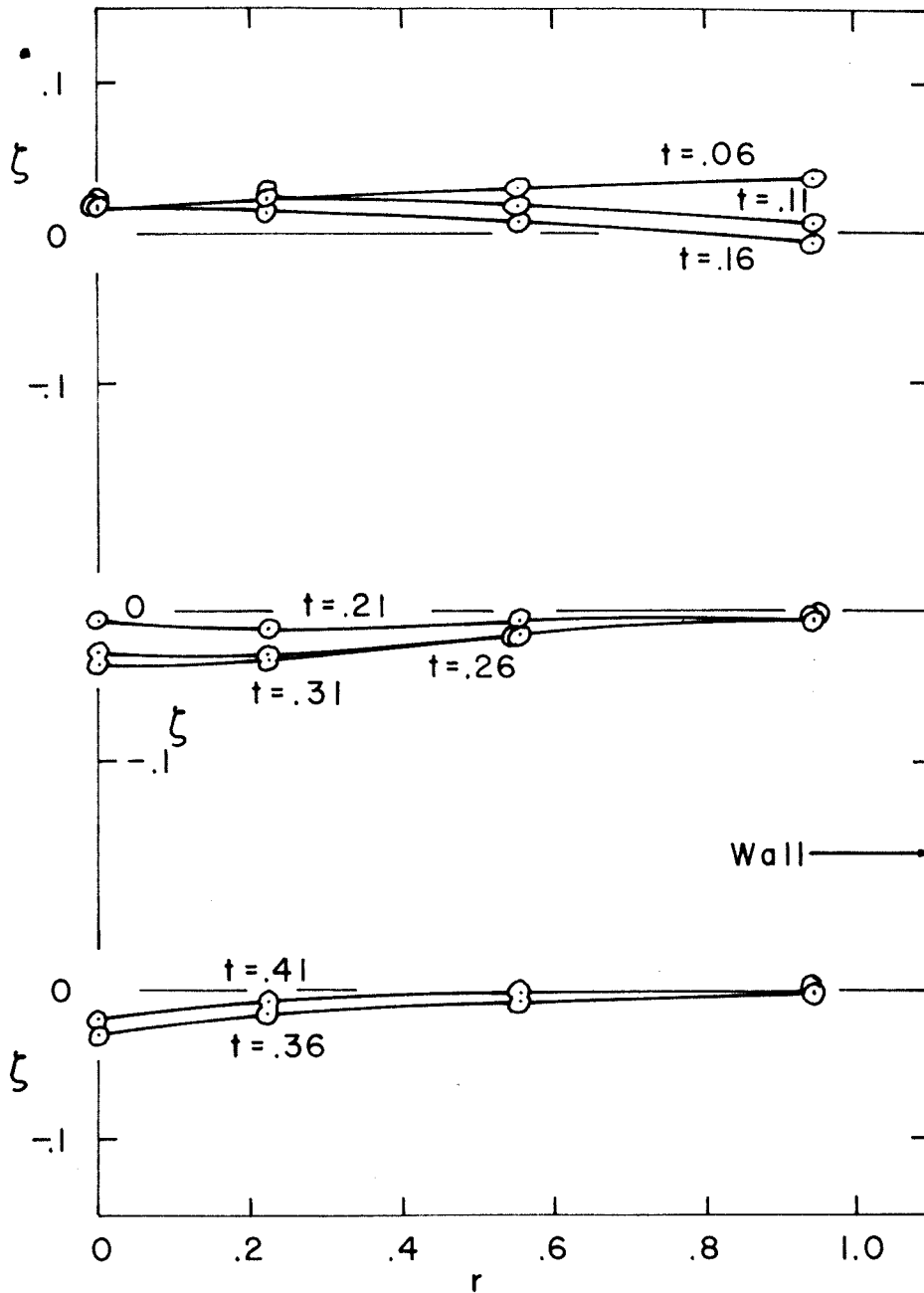


EXPERIMENTAL SURFACE DEFLECTIONS  
FIG. 6c



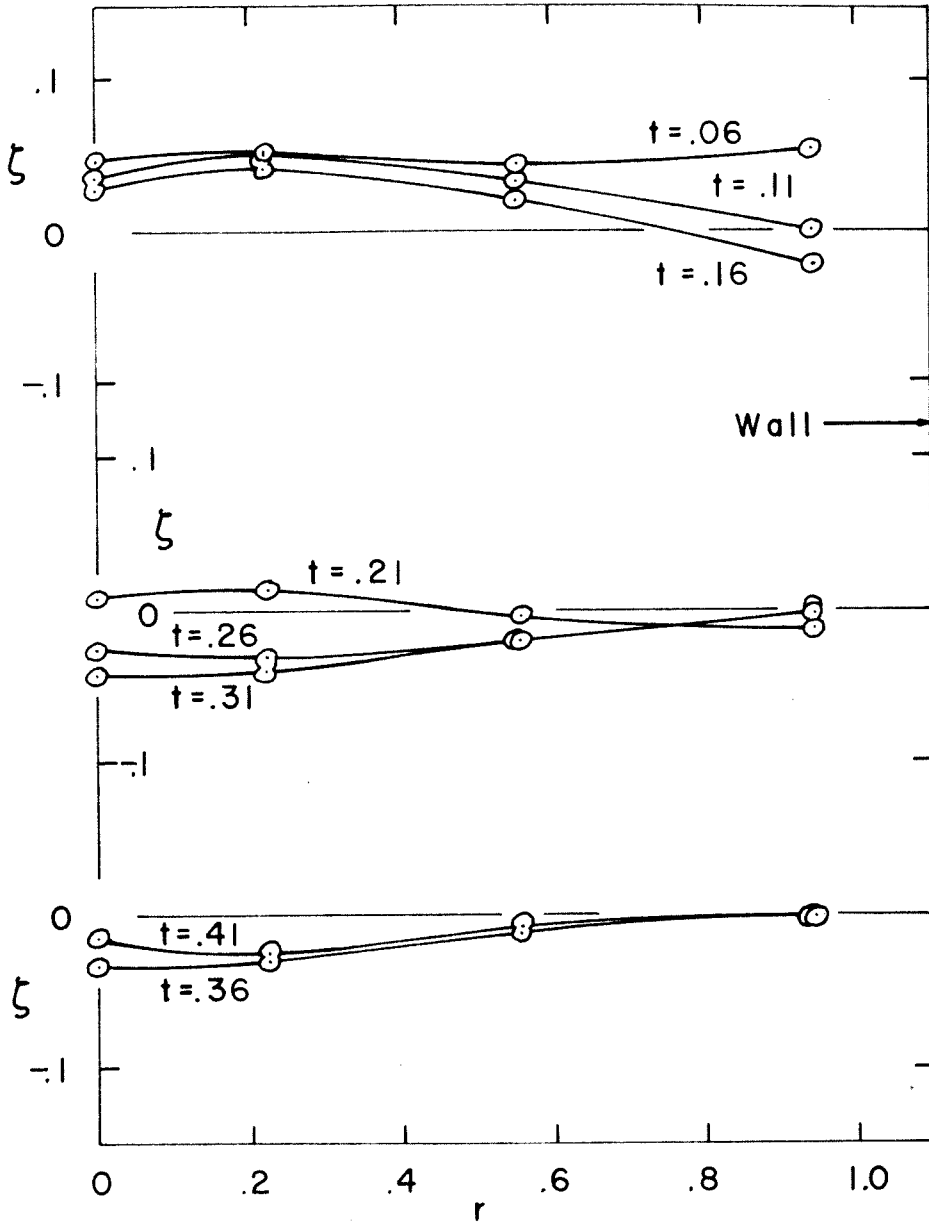


EXPERIMENTAL SURFACE DEFLECTIONS  
FIG. 7

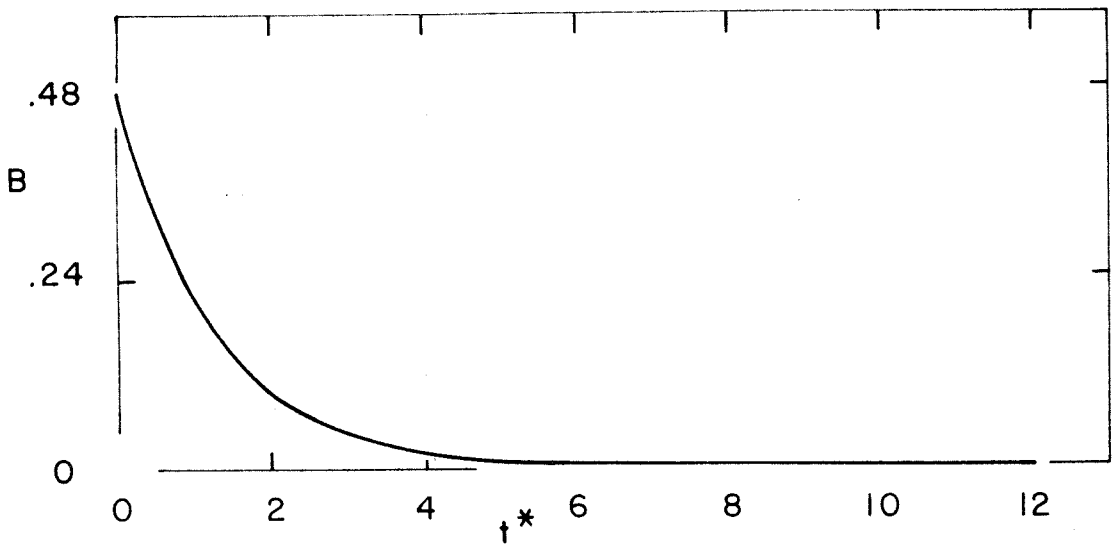
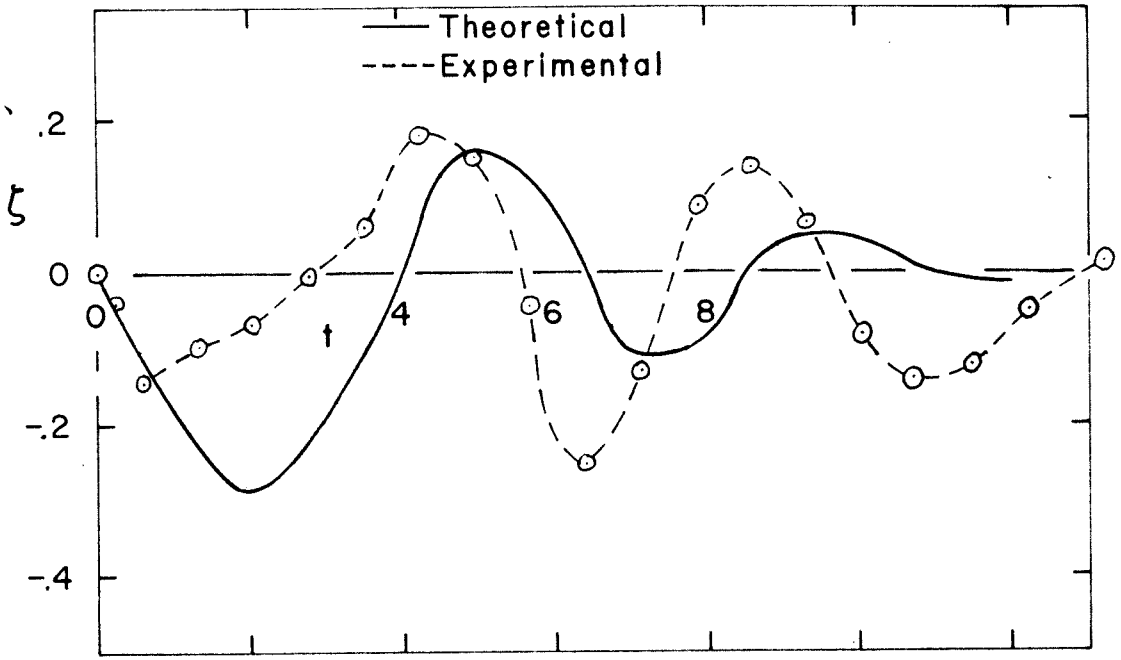


EXPERIMENTAL SURFACE DEFLECTIONS

FIG. 8

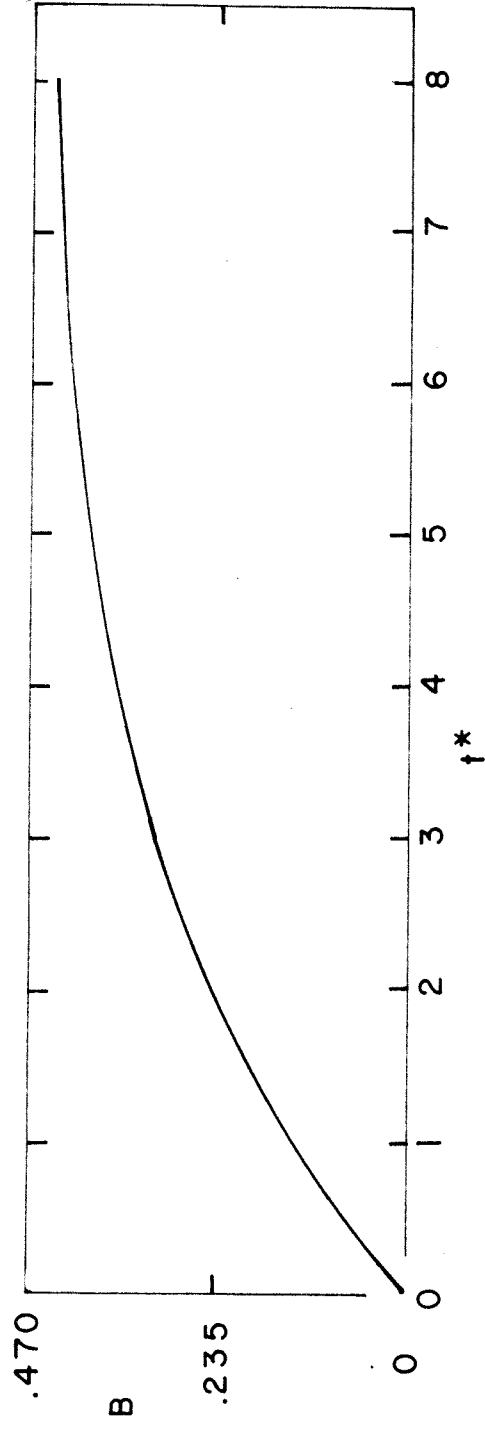
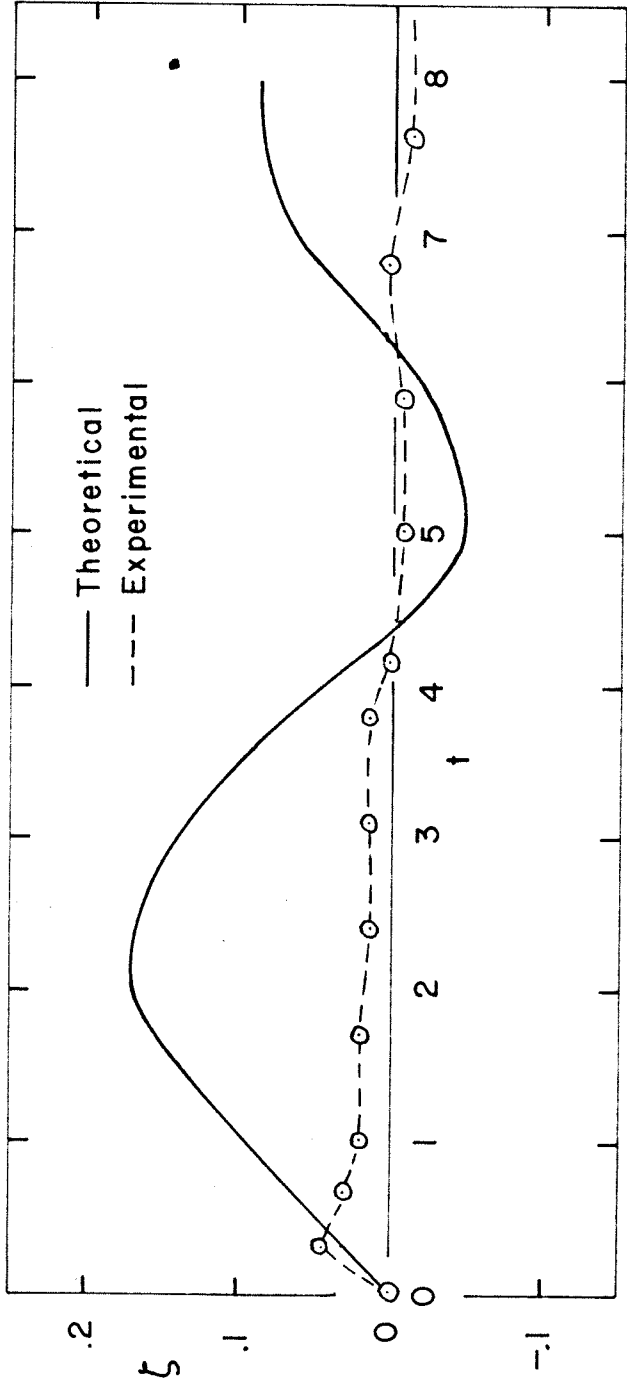


EXPERIMENTAL SURFACE DEFLECTIONS  
FIG. 9



COMPARISON OF THEORY AND EXPERIMENT  
SWITCHING OFF AT 4800 GAUSS (RUN 4)

FIG. 10



COMPARISON OF THEORY AND EXPERIMENT  
SWITCHING ON AT 4800 GAUSS (RUN 7)

FIG. 11